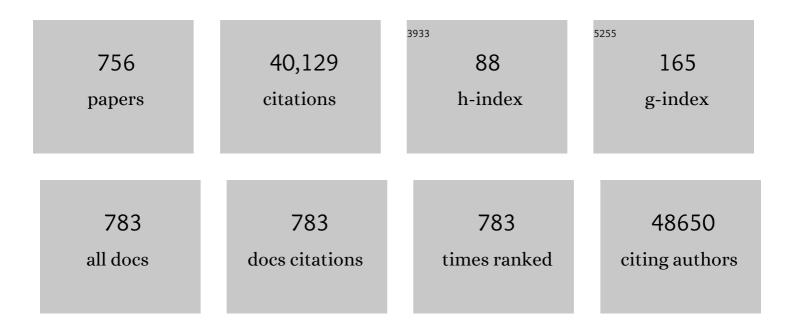
List of Publications by Year in descending order

Source: https://exaly.com/author-pdf/28247/publications.pdf Version: 2024-02-01



ΚΛΙΖΗΛΝΟ

#	Article	IF	CITATIONS
1	Forward Secure Public Key Encryption with Keyword Search for Outsourced Cloud Storage. IEEE Transactions on Cloud Computing, 2022, 10, 426-438.	4.4	40
2	Depression and insomnia in COVID-19 survivors: a cross-sectional survey from Chinese rehabilitation centers in Anhui province. Sleep Medicine, 2022, 91, 161-165.	1.6	40
3	Estimation of pollutant sources in multi-zone buildings through different deconvolution algorithms. Building Simulation, 2022, 15, 817-830.	5.6	11
4	Interrupted intramolecular donor-acceptor interaction compensated by strong through-space electronic coupling for highly efficient near-infrared TADF with emission over 800Ânm. Chemical Engineering Journal, 2022, 430, 132744.	12.7	23
5	A strategy combining 3D-DNA Walker and CRISPR-Cas12a trans-cleavage activity applied to MXene based electrochemiluminescent sensor for SARS-CoV-2 RdRp gene detection. Talanta, 2022, 236, 122868.	5.5	59
6	A pH-engineering regenerative DNA tetrahedron ECL biosensor for the assay of SARS-CoV-2 RdRp gene based on CRISPR/Cas12a trans-activity. Chemical Engineering Journal, 2022, 429, 132472.	12.7	49
7	Rational engineering the DNA tetrahedrons of dual wavelength ratiometric electrochemiluminescence biosensor for high efficient detection of SARS-CoV-2 RdRp gene by using entropy-driven and bipedal DNA walker amplification strategy. Chemical Engineering Journal, 2022, 427, 131686.	12.7	50
8	Cultural transmission based multi-objective evolution strategy for evolutionary multitasking. Information Sciences, 2022, 582, 215-242.	6.9	18
9	<i>H</i> _{â^ž} -Based Minimal Energy Adaptive Control With Preset Convergence Rate. IEEE Transactions on Cybernetics, 2022, 52, 10078-10088.	9.5	8
10	Residual Gated Dynamic Sparse Network for Gearbox Fault Diagnosis Using Multisensor Data. IEEE Transactions on Industrial Informatics, 2022, 18, 2264-2273.	11.3	22
11	Architecture Design and Flight Control of a Novel Octopus Shaped Multirotor Vehicle. IEEE Robotics and Automation Letters, 2022, 7, 311-317.	5.1	5
12	Positive isotope effect in thermally activated delayed fluorescence emitters based on deuterium-substituted donor units. Chemical Engineering Journal, 2022, 430, 132822.	12.7	21
13	An extended π-backbone for highly efficient near-infrared thermally activated delayed fluorescence with enhanced horizontal molecular orientation. Materials Horizons, 2022, 9, 772-779.	12.2	26
14	Experimental study on the performance of a tree-shaped mini-channel liquid cooling heat sink. Case Studies in Thermal Engineering, 2022, 30, 101780.	5.7	14
15	Building Homogenous Li ₂ TiO ₃ Coating Layer on Primary Particles to Stabilize Liâ€Rich Mnâ€Based Cathode Materials. Small, 2022, 18, e2106337.	10.0	42
16	Investigation of wet ammonia combustion characteristics using LES with finite-rate chemistry. Fuel, 2022, 311, 122422.	6.4	8
17	A QM/MM study on through space charge transfer-based thermally activated delayed fluorescence molecules in the solid state. Journal of Materials Chemistry C, 2022, 10, 517-531.	5.5	30
18	A Conditional Privacy-Preserving Certificateless Aggregate Signature Scheme in the Standard Model for VANETs. IEEE Access, 2022, 10, 15605-15618.	4.2	21

#	Article	IF	CITATIONS
19	Theoretical Study on the Light-Emitting Mechanism of Multifunctional Thermally Activated Delayed Fluorescence Molecules. Journal of Physical Chemistry C, 2022, 126, 2437-2446.	3.1	10
20	Structure–property relationship study of blue thermally activated delayed fluorescence molecules with different donor and position substitutions: theoretical perspective and molecular design. Journal of Materials Chemistry C, 2022, 10, 4723-4736.	5.5	17
21	Free energy cost to assemble superlattices of polymer-grafted nanoparticles. Soft Matter, 2022, 18, 640-647.	2.7	3
22	Machine learning models for outcome prediction of Chinese uveal melanoma patients: A 15â€year followâ€up study. Cancer Communications, 2022, 42, 273-276.	9.2	10
23	An MXeneâ€Based Metal Anode with Stepped Sodiophilic Gradient Structure Enables a Large Current Density for Rechargeable Na–O ₂ Batteries. Advanced Materials, 2022, 34, e2106565.	21.0	35
24	Inverted perovskite/silicon V-shaped tandem solar cells with 27.6% efficiency <i>via</i> self-assembled monolayer-modified nickel oxide layer. Journal of Materials Chemistry A, 2022, 10, 7251-7262.	10.3	24
25	Challenges and advances in wide-temperature rechargeable lithium batteries. Energy and Environmental Science, 2022, 15, 1711-1759.	30.8	138
26	Highly efficient thermally activated delayed fluorescence emitters with suppressed energy loss and a fast reverse intersystem crossing process. Journal of Materials Chemistry C, 2022, 10, 3685-3690.	5.5	3
27	Inverse analysis of critical current density in a bulk high-temperature superconducting undulator. Physical Review Accelerators and Beams, 2022, 25, .	1.6	2
28	Dissipation behaviors of granular balls in a shaken closed container. Mechanical Systems and Signal Processing, 2022, 172, 108986.	8.0	13
29	Study on the performance of a miniscale channel heat sink with Y-shaped unit channels based on entransy analysis. Applied Thermal Engineering, 2022, 209, 118295.	6.0	8
30	TmcA functions as a lysine 2-hydroxyisobutyryltransferase to regulate transcription. Nature Chemical Biology, 2022, 18, 142-151.	8.0	8
31	Regulating Pseudo-Jahn–Teller Effect and Superstructure in Layered Cathode Materials for Reversible Alkali-Ion Intercalation. Journal of the American Chemical Society, 2022, 144, 7929-7938.	13.7	22
32	Quinone Electrodes for Alkali–Acid Hybrid Batteries. Journal of the American Chemical Society, 2022, 144, 8066-8072.	13.7	23
33	Deepâ€Learningâ€Enabled Crack Detection and Analysis in Commercial Lithiumâ€Ion Battery Cathodes. Advanced Functional Materials, 2022, 32, .	14.9	9
34	Feature detection network-based correction method for accurate nano-tomography reconstruction. Applied Optics, 2022, 61, 5695.	1.8	3
35	Hysteresis Induced by Incomplete Cationic Redox in Liâ€Rich 3dâ€Transitionâ€Metal Layered Oxides Cathodes. Advanced Science, 2022, 9, .	11.2	7
36	Effect of roof and ceiling configuration on energy performance of a metamaterial-based cool roof for low-rise office building in China. Indoor and Built Environment, 2021, 30, 1739-1750.	2.8	7

#	Article	IF	CITATIONS
37	Evolution Strategy-Based Many-Objective Evolutionary Algorithm Through Vector Equilibrium. IEEE Transactions on Cybernetics, 2021, 51, 5455-5467.	9.5	20
38	Multi-Client Sub-Linear Boolean Keyword Searching for Encrypted Cloud Storage with Owner-Enforced Authorization. IEEE Transactions on Dependable and Secure Computing, 2021, 18, 2875-2887.	5.4	23
39	Efficacy of anticonvulsant ethosuximide for major depressive disorder: a randomized, placebo-control clinical trial. European Archives of Psychiatry and Clinical Neuroscience, 2021, 271, 487-493.	3.2	6
40	Analysis of the impact of a novel cool roof on cooling performance for a low-rise prefabricated building in China. Building Services Engineering Research and Technology, 2021, 42, 26-44.	1.8	26
41	Investigation of wet combustion instability due to bio-syngas fuel variability. Fuel, 2021, 285, 119120.	6.4	9
42	Systematic Proteome and Lysine Succinylome Analysis Reveals Enhanced Cell Migration by Hyposuccinylation in Esophageal Squamous Cell Carcinoma. Molecular and Cellular Proteomics, 2021, 20, 100053.	3.8	28
43	Peptide based Biosensing of Protein Functional Control Indicates Novel Mechanism of Cancerous Development under Oxidative Stress. Sensors and Actuators B: Chemical, 2021, 329, 129121.	7.8	2
44	Recent breakthroughs and perspectives of high-energy layered oxide cathode materials for lithium ion batteries. Materials Today, 2021, 43, 132-165.	14.2	174
45	Mitigation of Jahn–Teller distortion and Na ⁺ /vacancy ordering in a distorted manganese oxide cathode material by Li substitution. Chemical Science, 2021, 12, 1062-1067.	7.4	64
46	Optogenetically Controlled TrkA Activity Improves the Regenerative Capacity of Hairâ€Follicleâ€Đerived Stem Cells to Differentiate into Neurons and Glia. Advanced Biology, 2021, 5, 2000134.	2.5	6
47	A method for material decomposition and quantification with grating based phase CT. PLoS ONE, 2021, 16, e0245449.	2.5	3
48	Electrochemiluminescence platform for transcription factor diagnosis by using CRISPR–Cas12a <i>trans</i> -cleavage activity. Chemical Communications, 2021, 57, 8015-8018.	4.1	20
49	Positive impact of chromophore flexibility on the efficiency of red thermally activated delayed fluorescence materials. Materials Horizons, 2021, 8, 1297-1303.	12.2	41
50	Interfacial engineering facilitating robust Li _{6.35} Ga _{0.15} La ₃ Zr _{1.8} Nb _{0.2} O ₁₂ for all-solid-state lithium batteries. Sustainable Energy and Fuels, 2021, 5, 2077-2084.	4.9	10
51	Understanding the Mesoscale Degradation in Nickel-Rich Cathode Materials through Machine-Learning-Revealed Strain–Redox Decoupling. ACS Energy Letters, 2021, 6, 687-693.	17.4	42
52	Field Enhancing Model Predictive Direct Torque Control of Permanent Magnet Synchronous Machine. IEEE Transactions on Energy Conversion, 2021, 36, 2924-2933.	5.2	10
53	Fault Detection of Wind Turbines by Subspace Reconstruction-Based Robust Kernel Principal Component Analysis. IEEE Transactions on Instrumentation and Measurement, 2021, 70, 1-11.	4.7	13
54	Nickel doping as an effective strategy to promote separation of photogenerated charge carriers for efficient solar-fuel production. Catalysis Science and Technology, 2021, 11, 4012-4015.	4.1	8

#	Article	IF	CITATIONS
55	Highly efficient T-shaped deep-red thermally activated delayed fluorescence emitters: substitution position effect. Physical Chemistry Chemical Physics, 2021, 23, 21883-21892.	2.8	20
56	"Covalent biosensing―enables a one-step, reagent-less, low-cost and highly robust assay of SARS-CoV-2. Chemical Communications, 2021, 57, 10771-10774.	4.1	3
57	Electroless Formation of a Fluorinated Li/Na Hybrid Interphase for Robust Lithium Anodes. Journal of the American Chemical Society, 2021, 143, 2829-2837.	13.7	119
58	Highly Efficient Near-Infrared Thermally Activated Delayed Fluorescence Molecules via Acceptor Tuning: Theoretical Molecular Design and Experimental Verification. Journal of Physical Chemistry Letters, 2021, 12, 1893-1903.	4.6	48
59	Experimental and Numerical Investigation of Ultra-Wet Methane Combustion Technique for Power Generation. Journal of Engineering for Gas Turbines and Power, 2021, 143, .	1.1	6
60	Atomic arrangement matters: band-gap variation in composition-tunable (Ga1–xZnx)(N1–xOx) nanowires. Matter, 2021, 4, 1054-1071.	10.0	14
61	Self-esteem, social support and coping strategies of left-behind children in rural China, and the intermediary role of subjective support:a cross-sectional survey. BMC Psychiatry, 2021, 21, 158.	2.6	15
62	Entropy-driven electrochemiluminescence ultra-sensitive detection strategy of NF-κB p50 as the regulator of cytokine storm. Biosensors and Bioelectronics, 2021, 176, 112942.	10.1	22
63	Unifying the concepts of scattering and structure factor in ordered and disordered samples. Journal of Applied Crystallography, 2021, 54, 644-660.	4.5	2
64	Magnetization Current Simulation of High-Temperature Bulk Superconductors Using the ANSYS Iterative Algorithm Method. IEEE Transactions on Applied Superconductivity, 2021, 31, 1-6.	1.7	5
65	Structural Engineering of Covalent Organic Frameworks for Rechargeable Batteries. Advanced Energy Materials, 2021, 11, 2003054.	19.5	61
66	Zone plate-based full-field transmission X-ray microscopy beamline design at nearly diffraction-limited synchrotron radiation facility. Nuclear Instruments and Methods in Physics Research, Section A: Accelerators, Spectrometers, Detectors and Associated Equipment, 2021, 993, 165089.	1.6	1
67	Aromaticity/Antiaromaticity Effect on Activity of Transition Metal Macrocyclic Complexes towards Electrocatalytic Oxygen Reduction. ChemSusChem, 2021, 14, 1835-1839.	6.8	10
68	Rechargeable K O ₂ Batteries with a KSn Anode and a Carboxyl ontaining Carbon Nanotube Cathode Catalyst. Angewandte Chemie - International Edition, 2021, 60, 9540-9545.	13.8	23
69	High-capacity and small-polarization aluminum organic batteries based on sustainable quinone-based cathodes with Al3+ insertion. Cell Reports Physical Science, 2021, 2, 100354.	5.6	32
70	Effects of lysine 2-hydroxyisobutyrylation on bacterial Fabl activity and resistance to triclosan. Biochimie, 2021, 182, 197-205.	2.6	5
71	Sulfonated calix[4]arene functionalized SiO2@TiO2 for recognition of lysine methylation. Talanta, 2021, 224, 121819.	5.5	1
72	Quantifying Nanoparticle Assembly States in a Polymer Matrix through Deep Learning. Macromolecules, 2021, 54, 3034-3040.	4.8	9

#	Article	IF	CITATIONS
73	Entropy-driven amplified electrochemiluminescence biosensor for RdRp gene of SARS-CoV-2 detection with self-assembled DNA tetrahedron scaffolds. Biosensors and Bioelectronics, 2021, 178, 113015.	10.1	98
74	Highâ€Energyâ€Density Quinoneâ€Based Electrodes with [Al(OTF)] ²⁺ Storage Mechanism for Rechargeable Aqueous Aluminum Batteries. Advanced Functional Materials, 2021, 31, 2102063.	14.9	61
75	Rational Engineering of the DNA Walker Amplification Strategy by Using a Au@Ti ₃ C ₂ @PEI-Ru(dcbpy) ₃ ²⁺ Nanocomposite Biosensor for Detection of the SARS-CoV-2 RdRp Gene. ACS Applied Materials & Interfaces, 2021, 13, 19816-19824.	8.0	60
76	Opportunities and challenges for aqueous metal-proton batteries. Matter, 2021, 4, 1252-1273.	10.0	63
77	Finite rate simulations and analyses of wet/distributed flame structure in swirl-stabilized combustion. Fuel, 2021, 289, 119922.	6.4	13
78	Exploring the trans-cleavage activity of CRISPR-Cas12a for the development of a Mxene based electrochemiluminescence biosensor for the detection of Siglec-5. Biosensors and Bioelectronics, 2021, 178, 113019.	10.1	57
79	A Lowâ€Strain Potassiumâ€Rich Prussian Blue Analogue Cathode for High Power Potassiumâ€Ion Batteries. Angewandte Chemie - International Edition, 2021, 60, 13050-13056.	13.8	90
80	PHF8-promoted TOPBP1 demethylation drives ATR activation and preserves genome stability. Science Advances, 2021, 7, .	10.3	12
81	Experiences and Attitudes of Elementary School Students and Their Parents Toward Online Learning in China During the COVID-19 Pandemic: Questionnaire Study. Journal of Medical Internet Research, 2021, 23, e24496.	4.3	35
82	γ-Tocotrienol reverses multidrug resistance of breast cancer cells through the regulation of the γ-Tocotrienol-NF-κB-P-gp axis. Journal of Steroid Biochemistry and Molecular Biology, 2021, 209, 105835.	2.5	19
83	Cardiac cell type–specific gene regulatory programs and disease risk association. Science Advances, 2021, 7, .	10.3	63
84	Electrochemiluminescence aptasensor for Siglec-5 detection based on MoS2@Au nanocomposites emitter and exonuclease III-powered DNA walker. Sensors and Actuators B: Chemical, 2021, 334, 129592.	7.8	18
85	Hierarchical Ti ₃ C ₂ T _{<i>x</i>} MXene/Carbon Nanotubes for Low Overpotential and Long-Life Li-CO ₂ Batteries. ACS Nano, 2021, 15, 8407-8417.	14.6	54
86	Automatically Diagnosing Disk Bulge and Disk Herniation With Lumbar Magnetic Resonance Images by Using Deep Convolutional Neural Networks: Method Development Study. JMIR Medical Informatics, 2021, 9, e14755.	2.6	12
87	Advances and Challenges for the Electrochemical Reduction of CO ₂ to CO: From Fundamentals to Industrialization. Angewandte Chemie - International Edition, 2021, 60, 20627-20648.	13.8	408
88	Unexpected Role of Sterol Synthesis in RNA Stability and Translation in Leishmania. Biomedicines, 2021, 9, 696.	3.2	3
89	Nanoparticle-based fluorescence probe for detection of NF-κB transcription factor in single cell via steric hindrance. Mikrochimica Acta, 2021, 188, 226.	5.0	3
90	Regulating Electrocatalytic Oxygen Reduction Activity of a Metal Coordination Polymer via d–π Conjugation. Angewandte Chemie - International Edition, 2021, 60, 16937-16941.	13.8	74

#	Article	IF	CITATIONS
91	Engineering a self-navigated MnARK nanovaccine for inducing potent protective immunity against novel coronavirus. Nano Today, 2021, 38, 101139.	11.9	60
92	Sulfur-linked carbonyl polymer as a robust organic cathode for rapid and durable aluminum batteries. Journal of Energy Chemistry, 2021, 63, 320-327.	12.9	22
93	ERâ€anchored CRTH2 antagonizes collagen biosynthesis and organ fibrosis via binding LARP6. EMBO Journal, 2021, 40, e107403.	7.8	19
94	A hybrid attention improved ResNet based fault diagnosis method of wind turbines gearbox. Measurement: Journal of the International Measurement Confederation, 2021, 179, 109491.	5.0	93
95	Fault source location of wind turbine based on heterogeneous nodes complex network. Engineering Applications of Artificial Intelligence, 2021, 103, 104300.	8.1	14
96	Two-Stage Double Niched Evolution Strategy for Multimodal Multiobjective Optimization. IEEE Transactions on Evolutionary Computation, 2021, 25, 754-768.	10.0	26
97	Fully-staggered-array bulk Re-Ba-Cu-O short-period undulator: large-scale 3D electromagnetic modelling and design optimization using A-V and H-formulation methods. Superconductor Science and Technology, 2021, 34, 094002.	3.5	5
98	La,Al-Codoped SrTiO ₃ as a Photocatalyst in Overall Water Splitting: Significant Surface Engineering Effects on Defect Engineering. ACS Catalysis, 2021, 11, 11429-11439.	11.2	83
99	Two-Phase Transition Induced Amorphous Metal Phosphides Enabling Rapid, Reversible Alkali-Metal Ion Storage. ACS Nano, 2021, 15, 13486-13494.	14.6	23
100	Computerized assisted evaluation system for canine cardiomegaly via key points detection with deep learning. Preventive Veterinary Medicine, 2021, 193, 105399.	1.9	8
101	DNA-guided photoactivatable probe-based chemical proteomics reveals the reader protein of mRNA methylation. IScience, 2021, 24, 103046.	4.1	3
102	Insights into the Ionic Conduction Mechanism of Quasiâ€Solid Polymer Electrolytes through Multispectral Characterization. Angewandte Chemie, 2021, 133, 22854-22859.	2.0	5
103	Structures of outer-arm dynein array on microtubule doublet reveal a motor coordination mechanism. Nature Structural and Molecular Biology, 2021, 28, 799-810.	8.2	55
104	Designing Anionâ€Type Waterâ€Free Zn ²⁺ Solvation Structure for Robust Zn Metal Anode. Angewandte Chemie - International Edition, 2021, 60, 23357-23364.	13.8	179
105	Deep-learning-based image registration for nano-resolution tomographic reconstruction. Journal of Synchrotron Radiation, 2021, 28, 1909-1915.	2.4	9
106	Designing Anionâ€Type Waterâ€Free Zn ²⁺ Solvation Structure for Robust Zn Metal Anode. Angewandte Chemie, 2021, 133, 23545-23552.	2.0	57
107	Optogenetic Control of the Canonical Wnt Signaling Pathway During Xenopus laevis Embryonic Development. Journal of Molecular Biology, 2021, 433, 167050.	4.2	6
108	Accurate reconstruction algorithm for bilateral differential phase signals. Radiation Detection Technology and Methods, 2021, 5, 474-479.	0.8	1

#	Article	IF	CITATIONS
109	Insights into the Ionic Conduction Mechanism of Quasiâ€Solid Polymer Electrolytes through Multispectral Characterization. Angewandte Chemie - International Edition, 2021, 60, 22672-22677.	13.8	72
110	School Parks as a Community Health Resource: Use of Joint-Use Parks by Children before and during COVID-19 Pandemic. International Journal of Environmental Research and Public Health, 2021, 18, 9237.	2.6	11
111	An Improved Adaptive Selected Harmonic Elimination Algorithm for Current Measurement Error Correction of PMSMs. IEEE Transactions on Power Electronics, 2021, 36, 13128-13138.	7.9	17
112	A fault diagnosis method for wind turbines gearbox based on adaptive loss weighted meta-ResNet under noisy labels. Mechanical Systems and Signal Processing, 2021, 161, 107963.	8.0	75
113	Thiol-sensitive probe enables dynamic electrochemical assembly of serum protein for detecting SARS-Cov-2 marker protease in clinical samples. Biosensors and Bioelectronics, 2021, 194, 113579.	10.1	4
114	Advanced Transmission X-ray Microscopy for Energy Materials and Devices. , 2021, , 45-64.		0
115	Size-Sieving Separation of Hard-Sphere Gases at Low Concentrations through Cylindrically Porous Membranes. Soft Matter, 2021, 17, 10025-10031.	2.7	2
116	Constrained Feedback Control for Spacecraft Reorientation With an Optimal Gain. IEEE Transactions on Aerospace and Electronic Systems, 2021, 57, 3916-3926.	4.7	21
117	STOCHASTIC MODEL PREDICTIVE CONTROL FOR SPACECRAFT RENDEZVOUS AND DOCKING VIA A DISTRIBUTIONALLY ROBUST OPTIMIZATION APPROACH. ANZIAM Journal, 2021, 63, 39-57.	0.2	0
118	Automatic 3D image registration for nano-resolution chemical mapping using synchrotron spectro-tomography. Journal of Synchrotron Radiation, 2021, 28, 278-282.	2.4	11
119	Steering Molecular Activity with Optogenetics: Recent Advances and Perspectives. Advanced Biology, 2021, 5, e2000180.	2.5	13
120	Strategies for boosting carbon electrocatalysts for the oxygen reduction reaction in non-aqueous metal–air battery systems. Journal of Materials Chemistry A, 2021, 9, 6671-6693.	10.3	37
121	Fault Diagnosis of Wind Turbine Gearbox Using a Novel Method of Fast Deep Graph Convolutional Networks. IEEE Transactions on Instrumentation and Measurement, 2021, 70, 1-14.	4.7	52
122	In Situ Polymerized Conjugated Poly(pyreneâ€4,5,9,10â€ŧetraone)/Carbon Nanotubes Composites for Highâ€Performance Cathode of Sodium Batteries. Advanced Energy Materials, 2021, 11, 2002917.	19.5	69
123	Study on the Performance of a Y-Shaped Liquid Cooling Heat Sink Based on Constructal Law for Electronic Chip Cooling. Journal of Thermal Science and Engineering Applications, 2021, 13, .	1.5	6
124	The effect of Fe(<scp>iii</scp>) ions on oxygen-vacancy-rich BiVO ₄ on the photocatalytic oxygen evolution reaction. Catalysis Science and Technology, 2021, 11, 7598-7607.	4.1	7
125	Generalized Space-Code Index Modulation for High Rate and Energy-Efficient MIMO Transmission. IEEE Transactions on Vehicular Technology, 2021, 70, 12812-12820.	6.3	7
126	An atlas of gene regulatory elements in adult mouse cerebrum. Nature, 2021, 598, 129-136.	27.8	95

#	Article	IF	CITATIONS
127	Intermolecular interaction on excited-state properties of fluoro-substituted thermally activated delayed fluorescence molecules with aggregation-induced emission: a theoretical perspective. Molecular Physics, 2021, 119, e1862931.	1.7	3
128	Effects of Secondary Acceptors on Excited-State Properties of Sky-Blue Thermally Activated Delayed Fluorescence Molecules: Luminescence Mechanism and Molecular Design. Journal of Physical Chemistry A, 2021, 125, 175-186.	2.5	12
129	A single-cell atlas of chromatin accessibility in the human genome. Cell, 2021, 184, 5985-6001.e19.	28.9	194
130	Structural Isomerization Effect on the Triplet Energy Consumption Process of Organic Room-Temperature Phosphorescence Molecules: A QM/MM Study. Journal of Physical Chemistry C, 2021, 125, 27810-27819.	3.1	10
131	Lack of dopamine D1 receptors in the antidepressant actions of (R)-ketamine in a chronic social defeat stress model. European Archives of Psychiatry and Clinical Neuroscience, 2020, 270, 271-275.	3.2	15
132	Antibiotic-induced microbiome depletion is associated with resilience in mice after chronic social defeat stress. Journal of Affective Disorders, 2020, 260, 448-457.	4.1	67
133	Natural variation and selection in <i>GmSWEET39</i> affect soybean seed oil content. New Phytologist, 2020, 225, 1651-1666.	7.3	73
134	JMJD6 modulates DNA damage response through downregulating H4K16ac independently of its enzymatic activity. Cell Death and Differentiation, 2020, 27, 1052-1066.	11.2	13
135	Universal construction of ultrafine metal oxides coupled in N-enriched 3D carbon nanofibers for high-performance lithium/sodium storage. Nano Energy, 2020, 67, 104222.	16.0	51
136	Enabling Molecular Gapping and Bridging on a Biosensing Surface via Electrochemical Cross-Linking and Cleavage. Analytical Chemistry, 2020, 92, 2635-2641.	6.5	2
137	Effect of branching level on the performance of constructal theory based Y-shaped liquid cooling heat sink. Applied Thermal Engineering, 2020, 168, 114824.	6.0	38
138	An association study between methamphetamine use disorder with psychosis and polymorphisms in MiRNA. Neuroscience Letters, 2020, 717, 134725.	2.1	4
139	Molecular Orientation Determination in Nanodiscs at the Single-Molecule Level. Analytical Chemistry, 2020, 92, 2229-2236.	6.5	6
140	Impact of Electrostatic Interactions on the Self-Assembly of Charge-Neutral Block Copolyelectrolytes. Macromolecules, 2020, 53, 548-557.	4.8	14
141	Determination of the concentration of transcription factor by using exonuclease III-aided amplification and gold nanoparticle mediated fluorescence intensity: A new method for gene transcription related enzyme detection. Analytica Chimica Acta, 2020, 1104, 132-139.	5.4	12
142	Precoding-Aided Spatial Modulation With Dual-Polarized Antennas Over Correlated Channels. IEEE Communications Letters, 2020, 24, 676-680.	4.1	2
143	Engineering Solid Electrolyte Interphase on Red Phosphorus for Long-Term and High-Capacity Sodium Storage. Chemistry of Materials, 2020, 32, 448-458.	6.7	29
144	Identification of dual histone modification-binding protein interaction by combining mass spectrometry and isothermal titration calorimetric analysis. Journal of Advanced Research, 2020, 22, 35-46.	9.5	10

#	Article	lF	CITATIONS
145	Privacy-Preserving Locally Weighted Linear Regression Over Encrypted Millions of Data. IEEE Access, 2020, 8, 2247-2257.	4.2	3
146	Enabling Versatile Control of Molecular Activity with Small Molecules and Light. Journal of Molecular Biology, 2020, 432, 5209-5211.	4.2	0
147	Syntaxin Clustering and Optogenetic Control for Synaptic Membrane Fusion. Journal of Molecular Biology, 2020, 432, 4773-4782.	4.2	8
148	Exploring the Interfacial Chemistry between Zinc Anodes and Aqueous Electrolytes via an In Situ Visualized Characterization System. ACS Applied Materials & Interfaces, 2020, 12, 55476-55482.	8.0	58
149	Tolerant Sequential Model Predictive Direct Torque Control of Permanent Magnet Synchronous Machine Drives. IEEE Transactions on Transportation Electrification, 2020, 6, 1167-1176.	7.8	24
150	An Accurate Ensemble Forecasting Approach for Highly Dynamic Cloud Workload With VMD and R-Transformer. IEEE Access, 2020, 8, 115992-116003.	4.2	8
151	Featuring surface sodium storage properties of confined MoS2/bacterial cellulose-derived carbon nanofibers anode. Applied Surface Science, 2020, 530, 147261.	6.1	13
152	An extensive numerical study of the burning dynamics of wildland fuel using proposed configuration space. International Journal of Heat and Mass Transfer, 2020, 160, 120174.	4.8	4
153	Room-Temperature Flexible Quasi-Solid-State Rechargeable Na–O ₂ Batteries. ACS Central Science, 2020, 6, 1955-1963.	11.3	25
154	Comparative Determination of Cytotoxicity of Sub-10 nm Copper Nanoparticles to Prokaryotic and Eukaryotic Systems. ACS Applied Materials & amp; Interfaces, 2020, 12, 50203-50211.	8.0	9
155	Multifunctionalities of Graphene for Exploiting a Facile Conversion Reaction Route of Perovskite CoSnO ₃ for Highly Reversible Na Ion Storage. Journal of Physical Chemistry Letters, 2020, 11, 7988-7995.	4.6	5
156	Solid-State Effect Induced Thermally Activated Delayed Fluorescence with Tunable Emission: A Multiscale Study. Journal of Physical Chemistry A, 2020, 124, 8540-8550.	2.5	18
157	Scale-Resolving Simulation of a Propane-Fuelled Industrial Gas Turbine Combustor Using Finite-Rate Tabulated Chemistry. Fluids, 2020, 5, 126.	1.7	3
158	A feedforward circuit shaped by ECT2 and USP7 contributes to breast carcinogenesis. Theranostics, 2020, 10, 10769-10790.	10.0	12
159	Correspondence between Winding Numbers and Skin Modes in Non-Hermitian Systems. Physical Review Letters, 2020, 125, 126402.	7.8	428
160	Motto: Representing Motifs in Consensus Sequences with Minimum Information Loss. Genetics, 2020, 216, 353-358.	2.9	1
161	Modulating electrolyte structure for ultralow temperature aqueous zinc batteries. Nature Communications, 2020, 11, 4463.	12.8	431
162	A Universal Graphene Quantum Dot Tethering Design Strategy to Synthesize Singleâ€Atom Catalysts. Angewandte Chemie - International Edition, 2020, 59, 21885-21889.	13.8	79

#	Article	IF	CITATIONS
163	A Universal Graphene Quantum Dot Tethering Design Strategy to Synthesize Singleâ€Atom Catalysts. Angewandte Chemie, 2020, 132, 22069-22073.	2.0	9
164	Non-Hermitian Bulk-Boundary Correspondence and Auxiliary Generalized Brillouin Zone Theory. Physical Review Letters, 2020, 125, 226402.	7.8	245
165	Application of Multiplexed Aptasensors in Food Contaminants Detection. ACS Sensors, 2020, 5, 3721-3738.	7.8	75
166	A dual-labeling probe to track functional mitochondria–lysosome interactions in live cells. Nature Communications, 2020, 11, 6290.	12.8	116
167	Depth-dependent valence stratification driven by oxygen redox in lithium-rich layered oxide. Nature Communications, 2020, 11, 6342.	12.8	34
168	Simultaneous Road Surface and Centerline Extraction From Large-Scale Remote Sensing Images Using CNN-Based Segmentation and Tracing. IEEE Transactions on Geoscience and Remote Sensing, 2020, 58, 8919-8931.	6.3	84
169	Competition between PAF1 and MLL1/COMPASS confers the opposing function of LEDGF/p75 in HIV latency and proviral reactivation. Science Advances, 2020, 6, eaaz8411.	10.3	13
170	Solutions to mitigate the impact of measurement noise on the air pollution source strength estimation in a multi-zone building. Building Simulation, 2020, 13, 1329-1337.	5.6	9
171	The origin of heavy element doping to relieve the lattice thermal vibration of layered materials for high energy density Li ion cathodes. Journal of Materials Chemistry A, 2020, 8, 12424-12435.	10.3	37
172	HRP2–DPF3a–BAF complex coordinates histone modification and chromatin remodeling to regulate myogenic gene transcription. Nucleic Acids Research, 2020, 48, 6563-6582.	14.5	25
173	Oncoprotein SND1 hijacks nascent MHC-I heavy chain to ER-associated degradation, leading to impaired CD8 ⁺ T cell response in tumor. Science Advances, 2020, 6, .	10.3	18
174	Dense anatomical annotation of slit-lamp images improves the performance of deep learning for the diagnosis of ophthalmic disorders. Nature Biomedical Engineering, 2020, 4, 767-777.	22.5	42
175	Illustrating the Concepts of Entropy, Free Energy, and Thermodynamic Equilibrium with a Lattice Model. Journal of Chemical Education, 2020, 97, 1903-1907.	2.3	0
176	A Case Report of Suicide Attempt Caused by Acute and Transient Psychotic Disorder during the COVID-19 Outbreak. Case Reports in Psychiatry, 2020, 2020, 1-3.	0.5	8
177	Genetic Variation and Sequence Diversity of Starch Biosynthesis and Sucrose Metabolism Genes in Sweet Potato. Agronomy, 2020, 10, 627.	3.0	6
178	A 3D Hydroxylated MXene/Carbon Nanotubes Composite as a Scaffold for Dendriteâ€Free Sodiumâ€Metal Electrodes. Angewandte Chemie - International Edition, 2020, 59, 16705-16711.	13.8	138
179	A well-designed Gold nanoparticle based fluorescence probe for assay Argonaute2 and Let-7a interaction in living cells. Sensors and Actuators B: Chemical, 2020, 312, 128000.	7.8	5
180	Selective Growth of Stacking Fault Free ⟠100⟠© Nanowires on a Polycrystalline Substrate for Energy Conversion Application. ACS Applied Materials & Interfaces, 2020, 12, 17676-17685.	8.0	8

#	Article	IF	CITATIONS
181	An Integrated Approach for Combinatorial Readout of Dual Histone Modifications by Epigenetic Tandem Domains. Analytical Chemistry, 2020, 92, 6218-6223.	6.5	3
182	Chromatin accessibility and histone acetylation in the regulation of competence in early development. Developmental Biology, 2020, 462, 20-35.	2.0	29
183	Sub-ambient radiative cooling and its application in buildings. Building Simulation, 2020, 13, 1165-1189.	5.6	33
184	Early But Not Delayed Optogenetic RAF Activation Promotes Astrocytogenesis in Mouse Neural Progenitors. Journal of Molecular Biology, 2020, 432, 4358-4368.	4.2	8
185	Upconversion Nanoparticle-Induced Multimode Photodynamic Therapy Based on a Metal–Organic Framework/Titanium Dioxide Nanocomposite. ACS Applied Materials & Interfaces, 2020, 12, 12600-12608.	8.0	74
186	Dual-Wavelength Electrochemiluminescence Ratiometric Biosensor for NF-κB p50 Detection with Dimethylthiodiaminoterephthalate Fluorophore and Self-Assembled DNA Tetrahedron Nanostructures Probe. ACS Applied Materials & Interfaces, 2020, 12, 11409-11418.	8.0	54
187	Molecular investigation on the anomalous phenomenon at liquid desiccant surfaces for air conditioning. Building Simulation, 2020, 13, 599-608.	5.6	5
188	Diagnosing chronic atrophic gastritis by gastroscopy using artificial intelligence. Digestive and Liver Disease, 2020, 52, 566-572.	0.9	71
189	Essential role of microglial transforming growth factor-β1 in antidepressant actions of (R)-ketamine and the novel antidepressant TGF-β1. Translational Psychiatry, 2020, 10, 32.	4.8	75
190	Numerical Design Optimization of Short-Period HTS Staggered Array Undulators. IEEE Transactions on Applied Superconductivity, 2020, 30, 1-5.	1.7	9
191	Gas distribution mapping for indoor environments based on laser absorption spectroscopy: Development of an improved tomographic algorithm. Building and Environment, 2020, 172, 106724.	6.9	13
192	Electrodeposition Accelerates Metal-Based Batteries. Joule, 2020, 4, 10-11.	24.0	36
193	Molecular Design Strategy for Highâ€Redoxâ€Potential and Poorly Soluble nâ€Type Phenazine Derivatives as Cathode Materials for Lithium Batteries. ChemSusChem, 2020, 13, 2337-2344.	6.8	35
194	Datasets for high hydrogen content syngas fuel variability effect on combustion physicochemical properties. Data in Brief, 2020, 29, 105116.	1.0	0
195	A study of the canopy effect on fire regime transition using an objectively defined Byram convective number. Fire Safety Journal, 2020, 112, 102950.	3.1	5
196	Magnetization simulation of ReBCO tape stack with a large number of layers using the ANSYS A-V-A formulation. IEEE Transactions on Applied Superconductivity, 2020, , 1-1.	1.7	11
197	Coordinated Market Design for Peer-to-Peer Energy Trade and Ancillary Services in Distribution Grids. IEEE Transactions on Smart Grid, 2020, 11, 2929-2941.	9.0	134
198	Temperature and Rain Moderate the Effect of Neighborhood Walkability on Walking Time for Seniors in Barcelona. International Journal of Environmental Research and Public Health, 2020, 17, 14.	2.6	32

#	Article	IF	CITATIONS
199	Highly Reversible and Rapid Sodium Storage in GeP ₃ with Synergistic Effect from Outside-In Optimization. ACS Nano, 2020, 14, 4352-4365.	14.6	31
200	Robust Global Boundary Vibration Control of Uncertain Timoshenko Beam With Exogenous Disturbances. IEEE Access, 2020, 8, 72047-72058.	4.2	4
201	The Spread and Transmission of Sweet Potato Virus Disease (SPVD) and Its Effect on the Gene Expression Profile in Sweet Potato. Plants, 2020, 9, 492.	3.5	17
202	Self-Assembled Nucleotide/Saccharide-Tethering Polycation-Based Nanoparticle for Targeted Tumor Therapy. , 2020, 2, 550-556.		7
203	Association analysis between CAMKK2 rs1063843 and patients with schizophrenia in a Han Chinese population. Asian Journal of Psychiatry, 2020, 52, 102055.	2.0	0
204	A Generalizable Optogenetic Strategy to Regulate Receptor Tyrosine Kinases during Vertebrate Embryonic Development. Journal of Molecular Biology, 2020, 432, 3149-3158.	4.2	15
205	PHF20L1 as a H3K27me2 reader coordinates with transcriptional repressors to promote breast tumorigenesis. Science Advances, 2020, 6, eaaz0356.	10.3	26
206	Treatment concerns for psychiatric symptoms in patients with COVID-19 with or without psychiatric disorders. British Journal of Psychiatry, 2020, 217, 351-351.	2.8	41
207	Vortex breakdown of the swirling flow in a Lean Direct Injection burner. Physics of Fluids, 2020, 32, .	4.0	21
208	Fast and efficient critical state modelling of field-cooled bulk high-temperature superconductors using a backward computation method. Superconductor Science and Technology, 2020, 33, 114007.	3.5	12
209	Helical damping and dynamical critical skin effect in open quantum systems. Physical Review Research, 2020, 2, .	3.6	71
210	Dual phase grating based X-ray differential phase contrast imaging with source grating: theory and validation. Optics Express, 2020, 28, 9786.	3.4	17
211	Nucleation Mechanism and Substrate Modification of Lithium Metal Anode. Wuli Huaxue Xuebao/ Acta Physico - Chimica Sinica, 2020, .	4.9	3
212	Optical control of ERK and AKT signaling promotes axon regeneration and functional recovery of PNS and CNS in Drosophila. ELife, 2020, 9, .	6.0	23
213	Energy-Saving Analysis of Low-Rise Prefabricated Building Integrating with Metamaterial-Based Cool Roof in China. Environmental Science and Engineering, 2020, , 57-65.	0.2	1
214	Cloudâ€assisted secure and conjunctive publish/subscribe service in smart grids. IET Information Security, 2020, 14, 470-481.	1.7	3
215	Study on the Effects of Channel Deployment in a S-Shaped Liquid Cooling Heat Sink for Electronic Chip Cooling. Environmental Science and Engineering, 2020, , 87-95.	0.2	0
216	Numerical Study on Thermal Management of Data Center Integrated with Underfloor Vertical Baffles. Environmental Science and Engineering, 2020, , 77-85.	0.2	0

#	Article	IF	CITATIONS
217	Glass formation in binary alloys with different atomic symmetries. Physical Review Materials, 2020, 4, .	2.4	5
218	Efficient public key encryption with equality test in the standard model. Theoretical Computer Science, 2019, 755, 65-80.	0.9	41
219	In situ imaging and interfering Dicer-mediated cleavage process via a versatile molecular beacon probe. Analytica Chimica Acta, 2019, 1079, 146-152.	5.4	5
220	Public key encryption with equality test via hash proof system. Theoretical Computer Science, 2019, 795, 20-35.	0.9	10
221	LOXL2 Upregulates Phosphorylation of Ezrin to Promote Cytoskeletal Reorganization and Tumor Cell Invasion. Cancer Research, 2019, 79, 4951-4964.	0.9	47
222	A Framework for Multi-Regional Real-Time Pricing in Distribution Grids. IEEE Transactions on Smart Grid, 2019, 10, 6826-6838.	9.0	22
223	<p>Impact of serotonin transporter gene on rTMS augmentation of SSRIs for obsessive compulsive disorder</p> . Neuropsychiatric Disease and Treatment, 2019, Volume 15, 1771-1779.	2.2	15
224	Stable, predictable and training-free operation of superconducting Bi-2212 Rutherford cable racetrack coils at the wire current density of 1000 A/mm2. Scientific Reports, 2019, 9, 10170.	3.3	52
225	Protein lysine de-2-hydroxyisobutyrylation by CobB in prokaryotes. Science Advances, 2019, 5, eaaw6703.	10.3	51
226	Salt-controlled dissolution in pigment cathode for high-capacity and long-life magnesium organic batteries. Nano Energy, 2019, 65, 103902.	16.0	49
227	Influence of Electron Acceptor and Electron Donor on the Photophysical Properties of Carbon Dots: A Comparative Investigation at the Bulkâ€State and Singleâ€Particle Level. Advanced Functional Materials, 2019, 29, 1902466.	14.9	57
228	Regulation of EZH2 by SMYD2-Mediated Lysine Methylation Is Implicated in Tumorigenesis. Cell Reports, 2019, 29, 1482-1498.e4.	6.4	47
229	Repurposing Protein Degradation for Optogenetic Modulation of Protein Activities. ACS Synthetic Biology, 2019, 8, 2585-2592.	3.8	12
230	Conceptual design study of iron-based superconducting dipole magnets for SPPC. International Journal of Modern Physics A, 2019, 34, 1940003.	1.5	7
231	Ultrasensitive detection of transcription factors with a highly-efficient diaminoterephthalate fluorophore <i>via</i> an electrogenerated chemiluminescence strategy. Chemical Communications, 2019, 55, 11892-11895.	4.1	12
232	Theoretical Study of the Mechanism of Aggregation-Caused Quenching in Near-Infrared Thermally Activated Delayed Fluorescence Molecules: Hydrogen-Bond Effect. Journal of Physical Chemistry C, 2019, 123, 24705-24713.	3.1	89
233	Abnormal composition of gut microbiota is associated with resilience versus susceptibility to inescapable electric stress. Translational Psychiatry, 2019, 9, 231.	4.8	67
234	Peptide-Based Biosensing of Redox-Active Protein–Heme Complexes Indicates Novel Mechanism for Tumor Survival under Oxidative Stress. ACS Sensors, 2019, 4, 2671-2678.	7.8	5

#	Article	IF	CITATIONS
235	Bi-Based Z-Scheme Nanomaterials for the Photocatalytic Degradation of Organic Dyes. ACS Applied Nano Materials, 2019, 2, 6418-6427.	5.0	28
236	Uncertainty quantification of fuel variability effects on high hydrogen content syngas combustion. Fuel, 2019, 257, 116111.	6.4	19
237	Platelet-driven formation of interface peptide nano-network biosensor enabling a non-invasive means for early detection of Alzheimer's disease. Biosensors and Bioelectronics, 2019, 145, 111701.	10.1	19
238	A fluorometric aptamer method for kanamycin by applying a dual amplification strategy and using double Y-shaped DNA probes on a gold bar and onÂmagnetite nanoparticles. Mikrochimica Acta, 2019, 186, 120.	5.0	18
239	RNA chaperone assisted intramolecular annealing reaction towards oligouridylated RNA detection in cancer cells. Analyst, The, 2019, 144, 186-190.	3.5	0
240	Ultrathin carbon-coated FeS ₂ nanooctahedra for sodium storage with long cycling stability. Inorganic Chemistry Frontiers, 2019, 6, 459-464.	6.0	21
241	Conceptual design of TXM beamline at high energy photon source. AIP Conference Proceedings, 2019, , .	0.4	2
242	Dynamic output feedback sliding mode control for spacecraft hovering without velocity measurements. Journal of the Franklin Institute, 2019, 356, 1991-2014.	3.4	7
243	Quantification of Heterogeneous Degradation in Liâ€lon Batteries. Advanced Energy Materials, 2019, 9, 1900674.	19.5	176
244	Dietary intake of glucoraphanin prevents the reduction of dopamine transporter in the mouse striatum after repeated administration of MPTP. Neuropsychopharmacology Reports, 2019, 39, 247-251.	2.3	11
245	Fault diagnosis of planetary gearbox using a novel semi-supervised method of multiple association layers networks. Mechanical Systems and Signal Processing, 2019, 131, 243-260.	8.0	69
246	Inhibition of polycomb repressor complex 2 ameliorates neointimal hyperplasia by suppressing trimethylation of <scp>H3K27</scp> in vascular smooth muscle cells. British Journal of Pharmacology, 2019, 176, 3206-3219.	5.4	19
247	Dynamical source term estimation in a multi-compartment building under time-varying airflow. Building and Environment, 2019, 160, 106162.	6.9	28
248	Non-intrusive measurement method for the window opening behavior. Energy and Buildings, 2019, 197, 171-176.	6.7	21
249	The transcription factor FgMed1 is involved in early conidiogenesis and DON biosynthesis in the plant pathogenic fungus Fusarium graminearum. Applied Microbiology and Biotechnology, 2019, 103, 5851-5865.	3.6	5
250	Novel long-wavelength emissive lysosome-targeting ratiometric fluorescent probes for imaging in live cells. Analyst, The, 2019, 144, 4288-4294.	3.5	13
251	Dynamic Transcriptome Changes Related to Oil Accumulation in Developing Soybean Seeds. International Journal of Molecular Sciences, 2019, 20, 2202.	4.1	26
252	USP9X-mediated deubiquitination of B-cell CLL/lymphoma 9 potentiates Wnt signaling and promotes breast carcinogenesis. Journal of Biological Chemistry, 2019, 294, 9844-9857.	3.4	26

#	Article	IF	CITATIONS
253	Electromagnetic Design, Fabrication, and Test of LPF1: A 10.2-T Common-Coil Dipole Magnet With Graded Coil Configuration. IEEE Transactions on Applied Superconductivity, 2019, 29, 1-7.	1.7	10
254	Systemically modeling the relationship between climate change and wheat aphid abundance. Science of the Total Environment, 2019, 674, 392-400.	8.0	7
255	DNA Tetrahedron Based Biosensor for Argonaute2 Assay in Single Cells and Human Immunodeficiency Virus Type-1 Related Ribonuclease H Detection in Vitro. Analytical Chemistry, 2019, 91, 7086-7096.	6.5	30
256	Pseudocapacitive Behavior and Ultrafast Kinetics from Solvated Ion Cointercalation into MoS ₂ for Its Alkali Ion Storage. ACS Applied Energy Materials, 2019, 2, 3726-3735.	5.1	9
257	Comparison of antidepressant and side effects in mice after intranasal administration of (R,S)-ketamine, (R)-ketamine, and (S)-ketamine. Pharmacology Biochemistry and Behavior, 2019, 181, 53-59.	2.9	115
258	Key role of soluble epoxide hydrolase in the neurodevelopmental disorders of offspring after maternal immune activation. Proceedings of the National Academy of Sciences of the United States of America, 2019, 116, 7083-7088.	7.1	37
259	Energy Theft Detection With Energy Privacy Preservation in the Smart Grid. IEEE Internet of Things Journal, 2019, 6, 7659-7669.	8.7	131
260	Highâ€Voltage Chargingâ€Induced Strain, Heterogeneity, and Microâ€Cracks in Secondary Particles of a Nickelâ€Rich Layered Cathode Material. Advanced Functional Materials, 2019, 29, 1900247.	14.9	219
261	Zero background and triple-signal amplified fluorescence aptasensor for antibiotics detection in foods. Talanta, 2019, 199, 491-498.	5.5	17
262	Taiji: System-level identification of key transcription factors reveals transcriptional waves in mouse embryonic development. Science Advances, 2019, 5, eaav3262.	10.3	50
263	Novel functions of the ubiquitin-independent proteasome system in regulating <i>Xenopus</i> germline development. Development (Cambridge), 2019, 146, .	2.5	7
264	Ultrasensitive detection of hERG potassium channel in single-cell with photocleavable and entropy-driven reactions by using an electrochemical biosensor. Biosensors and Bioelectronics, 2019, 132, 310-318.	10.1	15
265	Nanoscale monitoring of mitochondria and lysosome interactions for drug screening and discovery. Nano Research, 2019, 12, 1009-1015.	10.4	45
266	Adaptive Optimal Control With Guaranteed Convergence Rate for Continuous-Time Linear Systems With Completely Unknown Dynamics. IEEE Access, 2019, 7, 11526-11532.	4.2	7
267	Airflow uniformity optimization for modular data center based on the constructal T-shaped underfloor air ducts. Applied Thermal Engineering, 2019, 155, 489-500.	6.0	24
268	Spatiotemporal Variations of Ambient Concentrations of Trace Elements in a Highly Polluted Region of China. Journal of Geophysical Research D: Atmospheres, 2019, 124, 4186-4202.	3.3	19
269	Beneficial effects of (R)-ketamine, but not its metabolite (2R,6R)-hydroxynorketamine, in the depression-like phenotype, inflammatory bone markers, and bone mineral density in a chronic social defeat stress model. Behavioural Brain Research, 2019, 368, 111904.	2.2	35
270	High pressure X-ray nano-tomography and fractal microstructures in the Ce Î ³ -α transition. Journal of Applied Physics, 2019, 125, 135902.	2.5	1

#	Article	IF	CITATIONS
271	New interfaces on MiD51 for Drp1 recruitment and regulation. PLoS ONE, 2019, 14, e0211459.	2.5	15
272	Integrative analysis with expanded DNA methylation data reveals common key regulators and pathways in cancers. Npj Genomic Medicine, 2019, 4, 2.	3.8	27
273	Microchip electrophoresis based aptasensor for multiplexed detection of antibiotics in foods via a stir-bar assisted multi-arm junctions recycling for signal amplification. Biosensors and Bioelectronics, 2019, 130, 139-146.	10.1	54
274	Combinatorial Peptide Ligand Library-Based Photoaffinity Probe for the Identification of Phosphotyrosine-Binding Domain Proteins. Analytical Chemistry, 2019, 91, 3221-3226.	6.5	4
275	Single-vesicle measurement of protein-induced membrane tethering. Colloids and Surfaces B: Biointerfaces, 2019, 177, 267-273.	5.0	4
276	Determination of the activity of uracil-DNA glycosylase by using two-tailed reverse transcription PCR and gold nanoparticle-mediated silver nanocluster fluorescence: a new method for gene therapy-related enzyme detection. Mikrochimica Acta, 2019, 186, 181.	5.0	8
277	Critical design factors for kinetically favorable P-based compounds toward alloying with Na ions for high-power sodium-ion batteries. Energy and Environmental Science, 2019, 12, 1326-1333.	30.8	58
278	Multilayer Tol Detection Approach for Nested NER. IEEE Access, 2019, 7, 186600-186608.	4.2	4
279	Multi-Authority Non-Monotonic KP-ABE With Cryptographic Reverse Firewall. IEEE Access, 2019, 7, 159002-159012.	4.2	13
280	Global Proteomic Analysis Reveals Widespread Lysine Succinylation in Rice Seedlings. International Journal of Molecular Sciences, 2019, 20, 5911.	4.1	10
281	Coaction of Electrostatic and Hydrophobic Interactions: Dynamic Constraints on Disordered TrkA Juxtamembrane Domain. Journal of Physical Chemistry B, 2019, 123, 10709-10717.	2.6	5
282	Structural basis of antagonism of human APOBEC3F by HIV-1 Vif. Nature Structural and Molecular Biology, 2019, 26, 1176-1183.	8.2	21
283	Development and validation of deep learning algorithms for scoliosis screening using back images. Communications Biology, 2019, 2, 390.	4.4	72
284	Detection of HIV-1 ribonuclease H activity in single-cell by using RNA mimics green fluorescent protein based biosensor. Sensors and Actuators B: Chemical, 2019, 281, 439-444.	7.8	12
285	Multiplexed electrochemical aptasensor for antibiotics detection using metallic-encoded apoferritin probes and double stirring bars-assisted target recycling for signal amplification. Talanta, 2019, 197, 491-499.	5.5	25
286	A Searchable Asymmetric Encryption Scheme with Support for Boolean Queries for Cloud Applications. Computer Journal, 2019, 62, 563-578.	2.4	15
287	Lack of Opioid System in the Antidepressant Actions of Ketamine. Biological Psychiatry, 2019, 85, e25-e27.	1.3	53
288	Bulk-state and single-particle imaging are central to understanding carbon dot photo-physics and elucidating the effects of precursor composition and reaction temperature. Carbon, 2019, 145, 572-585.	10.3	20

#	Article	IF	CITATIONS
289	Optogenetic Delineation of Receptor Tyrosine Kinase Subcircuits in PC12 Cell Differentiation. Cell Chemical Biology, 2019, 26, 400-410.e3.	5.2	31
290	Mechanical Design, Assembly, and Test of LPF1: A 10.2 T Nb ₃ Sn Common-Coil Dipole Magnet With Graded Coil Configuration. IEEE Transactions on Applied Superconductivity, 2019, 29, 1-8.	1.7	8
291	Entransy analysis on the performance of the counter-flow heat exchangers for a double evaporating temperature chiller. International Journal of Refrigeration, 2019, 98, 89-97.	3.4	5
292	Associations between the built environment and body mass index in the Mexican American Mano A Mano Cohort. Science of the Total Environment, 2019, 654, 456-462.	8.0	10
293	Increased expression of inwardly rectifying Kir4.1 channel in the parietal cortex from patients with major depressive disorder. Journal of Affective Disorders, 2019, 245, 265-269.	4.1	24
294	Impacts of cold weather on emergency hospital admission in Texas, 2004–2013. Environmental Research, 2019, 169, 139-146.	7.5	28
295	Manganese based layered oxides with modulated electronic and thermodynamic properties for sodium ion batteries. Nature Communications, 2019, 10, 5203.	12.8	202
296	Seasonal variation, formation mechanisms and potential sources of PM2.5 in two typical cities in the Central Plains Urban Agglomeration, China. Science of the Total Environment, 2019, 657, 657-670.	8.0	58
297	Deep learning PM2.5 concentrations with bidirectional LSTM RNN. Air Quality, Atmosphere and Health, 2019, 12, 411-423.	3.3	76
298	Increased BDNF-TrkB signaling in the nucleus accumbens plays a role in the risk for psychosis after cannabis exposure during adolescence. Pharmacology Biochemistry and Behavior, 2019, 177, 61-68.	2.9	7
299	Prediction of postoperative complications of pediatric cataract patients using data mining. Journal of Translational Medicine, 2019, 17, 2.	4.4	33
300	Effect of intermolecular interaction on excited-state properties of thermally activated delayed fluorescence molecules in solid phase: A QM/MM study. Spectrochimica Acta - Part A: Molecular and Biomolecular Spectroscopy, 2019, 209, 248-255.	3.9	12
301	An update on ketamine and its two enantiomers as rapid-acting antidepressants. Expert Review of Neurotherapeutics, 2019, 19, 83-92.	2.8	84
302	Lack of rapid antidepressant effects of Kir4.1 channel inhibitors in a chronic social defeat stress model: Comparison with (R)-ketamine. Pharmacology Biochemistry and Behavior, 2019, 176, 57-62.	2.9	15
303	Decomposition and Equilibrium Achieving Distribution Locational Marginal Prices Using Trust-Region Method. IEEE Transactions on Smart Grid, 2019, 10, 3269-3281.	9.0	41
304	Antibiotic-induced microbiome depletion protects against MPTP-induced dopaminergic neurotoxicity in the brain. Aging, 2019, 11, 6915-6929.	3.1	55
305	Reversible Optogenetic Control of Growth Factor Signaling During Cell Differentiation and Vertebrate Embryonic Development. , 2019, , .		0
306	An investigation of fuel variability effect on bio-syngas combustion using uncertainty quantification. Fuel, 2018, 220, 283-295.	6.4	17

#	Article	IF	CITATIONS
307	Lack of metabolism in (R)-ketamine's antidepressant actions in a chronic social defeat stress model. Scientific Reports, 2018, 8, 4007.	3.3	33
308	Security evaluation on Simeck against zero orrelation linear cryptanalysis. IET Information Security, 2018, 12, 87-93.	1.7	14
309	Swedish Nerve Growth Factor Mutation (NGF ^{R100W}) Defines a Role for TrkA and p75 ^{NTR} in Nociception. Journal of Neuroscience, 2018, 38, 3394-3413.	3.6	34
310	Microfluidic electrophoretic non-enzymatic kanamycin assay making use of a stirring bar functionalized with gold-labeled aptamer, of a fluorescent DNA probe, and of signal amplification via hybridization chain reaction. Mikrochimica Acta, 2018, 185, 181.	5.0	27
311	3D Mechanical Design and Stress Analysis of 20 T Common-Coil Dipole Magnet for SppC. IEEE Transactions on Applied Superconductivity, 2018, 28, 1-5.	1.7	9
312	An Integrated Approach Based on a DNA Self-Assembly Technique for Characterization of Crosstalk among Combinatorial Histone Modifications. Analytical Chemistry, 2018, 90, 3692-3696.	6.5	12
313	In Situ Visualization of hERG Potassium Channel via Dual Signal Amplification. Analytical Chemistry, 2018, 90, 6199-6205.	6.5	19
314	Remarkable Enhancement in Sodiumâ€lon Kinetics of NaFe ₂ (CN) ₆ by Chemical Bonding with Graphene. Small Methods, 2018, 2, 1700346.	8.6	40
315	Predicting daily PM2.5 concentrations in Texas using high-resolution satellite aerosol optical depth. Science of the Total Environment, 2018, 631-632, 904-911.	8.0	36
316	Bifunctional Conducting Polymer Coated CoP Core–Shell Nanowires on Carbon Paper as a Freeâ€5tanding Anode for Sodium Ion Batteries. Advanced Energy Materials, 2018, 8, 1800283.	19.5	104
317	Oncoprotein Tudor-SN is a key determinant providing survival advantage under DNA damaging stress. Cell Death and Differentiation, 2018, 25, 1625-1637.	11.2	23
318	A Secure Data Forwarding Protocol for Data Statistic Services in Multi-Hop Marine Sensor Networks*. Fundamenta Informaticae, 2018, 157, 63-78.	0.4	0
319	Maltose-Functionalized Hydrophilic Magnetic Nanoparticles with Polymer Brushes for Highly Selective Enrichment of N-Linked Glycopeptides. ACS Omega, 2018, 3, 1572-1580.	3.5	33
320	Interleukinâ€6 contributes to chemoresistance in MDAâ€MBâ€231 cells via targeting HIFâ€1α. Journal of Biochemical and Molecular Toxicology, 2018, 32, e22039.	3.0	40
321	Exergy and energy analysis of a double evaporating temperature chiller. Energy and Buildings, 2018, 165, 464-471.	6.7	15
322	Systematic Identification of Lysine 2-hydroxyisobutyrylated Proteins in Proteus mirabilis. Molecular and Cellular Proteomics, 2018, 17, 482-494.	3.8	43
323	A facile approach to constructing efficiently segregated conductive networks in poly(lactic) Tj ETQq1 1 0.784314 shielding. Composites Science and Technology, 2018, 156, 136-143.	rgBT /Ove 7.8	erlock 10 Tf 131
324	5-Hydroxytryptamine-Independent Antidepressant Actions of (R)-Ketamine in a Chronic Social Defeat Stress Model. International Journal of Neuropsychopharmacology, 2018, 21, 157-163.	2.1	43

#	Article	IF	CITATIONS
325	A brief introduction of cryo-EM revolution—the Nobel Prize in Chemistry 2017. Science China Life Sciences, 2018, 61, 368-370.	4.9	6
326	Yes-Associated Protein Promotes Angiogenesis via Signal Transducer and Activator of Transcription 3 in Endothelial Cells. Circulation Research, 2018, 122, 591-605.	4.5	98
327	Synthesis and characterization of novel push-pull oligomer based on naphthodithiophene-benzothiodiazole for OFETs application. Tetrahedron Letters, 2018, 59, 641-644.	1.4	2
328	Quench Detection Utilizing Stray Capacitances. IEEE Transactions on Applied Superconductivity, 2018, 28, 1-5.	1.7	13
329	USP52 acts as a deubiquitinase and promotes histone chaperone ASF1A stabilization. Nature Communications, 2018, 9, 1285.	12.8	33
330	Impact of aerobic exercise on cognitive impairment and oxidative stress markers in methamphetamine-dependent patients. Psychiatry Research, 2018, 266, 328-333.	3.3	30
331	Deletion of serine racemase confers D-serine –dependent resilience to chronic social defeat stress. Neurochemistry International, 2018, 116, 43-51.	3.8	18
332	Quench simulation results for a 12-T twin-aperture dipole magnet. Cryogenics, 2018, 92, 13-19.	1.7	6
333	A two dimensional metal–organic framework nanosheets-based fluorescence resonance energy transfer aptasensor with circular strand-replacement DNA polymerization target-triggered amplification strategy for homogenous detection of antibiotics. Analytica Chimica Acta, 2018, 1020, 1-8.	5.4	60
334	Uniform fiber orientation and transcrystallization formed in isotactic polypropylene/short glass fiber composites via a shearâ€induced orientation extrusion. Polymer Composites, 2018, 39, 3168-3177.	4.6	8
335	Triggering p53 activation is essential in ziyuglycoside lâ€induced human retinoblastoma WERIâ€Rbâ€1 cell apoptosis. Journal of Biochemical and Molecular Toxicology, 2018, 32, e22001.	3.0	10
336	Experimental studies of tuned particle damper: Design and characterization. Mechanical Systems and Signal Processing, 2018, 99, 219-228.	8.0	25
337	Recent Developments on and Prospects for Electrode Materials with Hierarchical Structures for Lithiumâ€lon Batteries. Advanced Energy Materials, 2018, 8, 1701415.	19.5	436
338	NUPR1 maintains autolysosomal efflux by activating <i>SNAP25</i> transcription in cancer cells. Autophagy, 2018, 14, 654-670.	9.1	70
339	Synchrotron Radiation Nanoscale X-ray Imaging Technology And Scientific Big Data Mining Assist Energy Materials Research. Microscopy and Microanalysis, 2018, 24, 542-543.	0.4	0
340	Defining the optimal criterion for separating gases using polymeric membranes. Soft Matter, 2018, 14, 9847-9850.	2.7	1
341	Chemical physics in living cells — Using light to visualize and control intracellular signal transduction. Chinese Journal of Chemical Physics, 2018, 31, 375-392.	1.3	0
342	Adaptive slidingâ€mode control for spacecraft relative position tracking with maneuvering target. International Journal of Robust and Nonlinear Control, 2018, 28, 5786-5810.	3.7	17

#	Article	IF	CITATIONS
343	Spleen tyrosine kinase SYK (L) interacts with YY 1 and coordinately suppresses SNAI 2 transcription in lung cancer cells. FEBS Journal, 2018, 285, 4229-4245.	4.7	15
344	Predicting the progression of ophthalmic disease based on slit-lamp images using a deep temporal sequence network. PLoS ONE, 2018, 13, e0201142.	2.5	18
345	A Sunlight Powered Portable Photoelectrochemical Biosensor Based on a Potentiometric Resolve Ratiometric Principle. Analytical Chemistry, 2018, 90, 13207-13211.	6.5	49
346	P <mml:math <br="" display="inline" overflow="scroll" xmlns:mml="http://www.w3.org/1998/Math/MathML">id="d1e1054" altimg="si7.gif"><mml:msup><mml:mrow /><mml:mrow><mml:mn>3</mml:mn></mml:mrow></mml:mrow </mml:msup></mml:math> GQ: A practical privacy-preserving generic location-based services query scheme. Pervasive and Mobile Computing,	3.3	10
347	2018, 51, 56-72. Comparison of rapid and long-lasting antidepressant effects of negative modulators of α5-containing GABAA receptors and (R)†ketamine in a chronic social defeat stress model. Pharmacology Biochemistry and Behavior, 2018, 175, 139-145.	2.9	19
348	Lack of deuterium isotope effects in the antidepressant effects of (R)-ketamine in a chronic social defeat stress model. Psychopharmacology, 2018, 235, 3177-3185.	3.1	29
349	An Efficient Approach for Selective Enrichment of Histone Modification Readers Using Self-Assembled Multivalent Photoaffinity Peptide Probes. Analytical Chemistry, 2018, 90, 11385-11392.	6.5	12
350	All Carbon Dual Ion Batteries. ACS Applied Materials & amp; Interfaces, 2018, 10, 35978-35983.	8.0	93
351	Tripled critical current in racetrack coils made of Bi-2212 Rutherford cables with overpressure processing and leakage control. Superconductor Science and Technology, 2018, 31, 105009.	3.5	26
352	Energy saving and economic analysis of a new hybrid radiative cooling system for single-family houses in the USA. Applied Energy, 2018, 224, 371-381.	10.1	112
353	Structure-property relationships of benzo[2,1- b :3,4- b '] bis [1]benzothiophenes for organic field effect transistors. Tetrahedron Letters, 2018, 59, 2717-2721.	1.4	3
354	An assessment of fuel variability effect on biogas-hydrogen combustion using uncertainty quantification. International Journal of Hydrogen Energy, 2018, 43, 12499-12515.	7.1	26
355	An endonuclease-linked multiplex immunoassay for tumor markers detection based on microfluidic chip electrophoresis for DNA analysis. Sensors and Actuators B: Chemical, 2018, 272, 526-533.	7.8	24
356	GeP3 with soft and tunable bonding nature enabling highly reversible alloying with Na ions. Materials Today Energy, 2018, 9, 126-136.	4.7	31
357	A sensitive RNA chaperone assay using induced RNA annealing by duplex specific nuclease for amplification. Analytica Chimica Acta, 2018, 1033, 199-204.	5.4	0
358	Pipecolic acid confers systemic immunity by regulating free radicals. Science Advances, 2018, 4, eaar4509.	10.3	115
359	Recent advancements on thermal management and evaluation for data centers. Applied Thermal Engineering, 2018, 142, 215-231.	6.0	75
360	Towards dynamic structure of biological complexes at atomic resolution by cryo-EM. Chinese Physics B, 2018, 27, 066801.	1.4	0

#	Article	IF	CITATIONS
361	Sensitive detection of cytokine in complex biological samples by using MB track mediated DNA walker and nicking enzyme assisted signal amplification method combined biosensor. Talanta, 2018, 189, 122-128.	5.5	18
362	Interlayer‧pacingâ€Regulated VOPO ₄ Nanosheets with Fast Kinetics for Highâ€Capacity and Durable Rechargeable Magnesium Batteries. Advanced Materials, 2018, 30, e1801984.	21.0	171
363	Direct observation of the kinetics of gas–solid reactions using <i>in situ</i> kinetic and spectroscopic techniques. Reaction Chemistry and Engineering, 2018, 3, 668-675.	3.7	8
364	The combined effect of ambient ozone exposure and toxic air releases on hospitalization for asthma among children in Harris County, Texas. International Journal of Environmental Health Research, 2018, 28, 358-378.	2.7	4
365	Finding relevant biomedical datasets: the UC San Diego solution for the bioCADDIE Retrieval Challenge. Database: the Journal of Biological Databases and Curation, 2018, 2018, .	3.0	8
366	Role of Inflammatory Bone Markers in the Antidepressant Actions of (R)-Ketamine in a Chronic Social Defeat Stress Model. International Journal of Neuropsychopharmacology, 2018, 21, 1025-1030.	2.1	12
367	Proteomic analysis of the OGT interactome: novel links to epithelial–mesenchymal transition and metastasis of cervical cancer. Carcinogenesis, 2018, 39, 1222-1234.	2.8	53
368	Lattice-Based Dual Receiver Encryption and More. Lecture Notes in Computer Science, 2018, , 520-538.	1.3	2
369	Assessing Heat Stress and Health among Construction Workers in a Changing Climate: A Review. International Journal of Environmental Research and Public Health, 2018, 15, 247.	2.6	137
370	Bayesian Networks Predict Neuronal Transdifferentiation. G3: Genes, Genomes, Genetics, 2018, 8, 2501-2511.	1.8	5
371	Propagation topography of redox phase transformations in heterogeneous layered oxide cathode materials. Nature Communications, 2018, 9, 2810.	12.8	59
372	Size-dependent penetrant diffusion in polymer glasses. Soft Matter, 2018, 14, 4226-4230.	2.7	22
373	Lack of antidepressant effects of low-voltage-sensitive T-type calcium channel blocker ethosuximide in a chronic social defeat stress model: Comparison with (R)-ketamine. International Journal of Neuropsychopharmacology, 2018, 21, 1031-1036.	2.1	15
374	Preliminary Study on High-sensitive Diffraction Enhanced Imaging at BSRF. Microscopy and Microanalysis, 2018, 24, 102-103.	0.4	0
375	Carbon dots with induced surface oxidation permits imaging at single-particle level for intracellular studies. Nanoscale, 2018, 10, 18510-18519.	5.6	26
376	Excitation characteristics of magnets impregnated with paraffin wax. Cryogenics, 2018, 94, 22-25.	1.7	4
377	Stable Carbon–Selenium Bonds for Enhanced Performance in <i>Tremella</i> â€Like 2D Chalcogenide Battery Anode. Advanced Energy Materials, 2018, 8, 1800927.	19.5	68
378	Security Analysis and Modification of ID-Based Encryption with Equality Test from ACISP 2017. Lecture Notes in Computer Science, 2018, , 780-786.	1.3	10

#	Article	IF	CITATIONS
379	Ubiquitin-specific protease 7 sustains DNA damage response and promotes cervical carcinogenesis. Journal of Clinical Investigation, 2018, 128, 4280-4296.	8.2	84
380	Polyphyllin I Induces Cell Cycle Arrest and Cell Apoptosis in Human Retinoblastoma Y-79 Cells through Targeting p53. Anti-Cancer Agents in Medicinal Chemistry, 2018, 18, 875-881.	1.7	16
381	An Interpretable and Expandable Deep Learning Diagnostic System for Multiple Ocular Diseases: Qualitative Study. Journal of Medical Internet Research, 2018, 20, e11144.	4.3	41
382	Adaptive weighted total variation regularized phase retrieval in differential phase-contrast imaging. Optical Engineering, 2018, 57, 1.	1.0	1
383	A Time Delay Compensation Method Based on Area Equivalence For Active Damping of an <italic>LCL</italic> -Type Converter. IEEE Transactions on Power Electronics, 2017, 32, 762-772.	7.9	134
384	A reduced graphene oxide-encapsulated phosphorus/carbon composite as a promising anode material for high-performance sodium-ion batteries. Journal of Materials Chemistry A, 2017, 5, 3683-3690.	10.3	54
385	Electromagnetic Design Study of a 20-T Cos-Theta 2-in-1 Dipole Magnet for High-Energy Accelerators. IEEE Transactions on Applied Superconductivity, 2017, 27, 1-5.	1.7	6
386	Ultralow Percolation Threshold in Poly(<scp>l</scp> -lactide)/Poly(Îμ-caprolactone)/Multiwall Carbon Nanotubes Composites with a Segregated Electrically Conductive Network. Journal of Physical Chemistry C, 2017, 121, 3087-3098.	3.1	83
387	DNA-Templated Aptamer Probe for Identification of Target Proteins. Analytical Chemistry, 2017, 89, 4071-4076.	6.5	22
388	Morphological regulation improved electrical conductivity and electromagnetic interference shielding in poly(<scp>l</scp> -lactide)/poly(ε-caprolactone)/carbon nanotube nanocomposites via constructing stereocomplex crystallites. Journal of Materials Chemistry C, 2017, 5, 2807-2817.	5.5	144
389	Comparative analysis of image classification methods for automatic diagnosis of ophthalmic images. Scientific Reports, 2017, 7, 41545.	3.3	41
390	Serum proteomic-based analysis identifying autoantibodies against PRDX2 and PRDX3 as potential diagnostic biomarkers in nasopharyngeal carcinoma. Clinical Proteomics, 2017, 14, 6.	2.1	22
391	Impacts of cold weather on all-cause and cause-specific mortality in Texas, 1990–2011. Environmental Pollution, 2017, 225, 244-251.	7.5	37
392	Crystallization kinetics and morphology of biodegradable Poly(Îμ-caprolactone) with chain-like distribution of ferroferric oxide nanoparticles: Toward mechanical enhancements. Polymer, 2017, 117, 84-95.	3.8	11
393	Sonocatalytic degradation of organic pollutant by SnO 2 /MWCNT nanocomposite. Diamond and Related Materials, 2017, 76, 177-183.	3.9	27
394	Ultrasensitive fluorescence detection of transcription factors based on kisscomplex formation and the T7 RNA polymerase amplification method. Chemical Communications, 2017, 53, 5846-5849.	4.1	18
395	In-situ synthesis and textural evolution of the novel carbonaceous SiC/mullite aerogel via polymer-derived ceramics route. Ceramics International, 2017, 43, 9896-9905.	4.8	12
396	In situ Visualization of State-of-Charge Heterogeneity within a LiCoO ₂ Particle that Evolves upon Cycling at Different Rates. ACS Energy Letters, 2017, 2, 1240-1245.	17.4	159

#	Article	IF	CITATIONS
397	Regulation and imaging of gene expression via an RNA interference antagonistic biomimetic probe. Chemical Science, 2017, 8, 4973-4977.	7.4	18
398	Characterizing spatial variability of air pollution from vehicle traffic around the Houston Ship Channel area. Atmospheric Environment, 2017, 161, 167-175.	4.1	30
399	Enhanced electrical conductivity and piezoresistive sensing in multi-wall carbon nanotubes/polydimethylsiloxane nanocomposites via the construction of a self-segregated structure. Nanoscale, 2017, 9, 11017-11026.	5.6	179
400	Stable small bubble clusters in two-dimensional foams. Soft Matter, 2017, 13, 4370-4380.	2.7	1
401	An improved ripple suppression method based on flying-capacitor modular multilevel converter for high performance MV drivers. , 2017, , .		2
402	Cryo-EM Reveals How Human Cytoplasmic Dynein Is Auto-inhibited and Activated. Cell, 2017, 169, 1303-1314.e18.	28.9	237
403	A decision tree–based combination of ezrin-interacting proteins to estimate the prognostic risk of patients with esophageal squamous cell carcinoma. Human Pathology, 2017, 66, 115-125.	2.0	12
404	Puerarin inhibits amyloid β-induced NLRP3 inflammasome activation in retinal pigment epithelial cells via suppressing ROS-dependent oxidative and endoplasmic reticulum stresses. Experimental Cell Research, 2017, 357, 335-340.	2.6	56
405	Structural and chemical synergistic effect of CoS nanoparticles and porous carbon nanorods for high-performance sodium storage. Nano Energy, 2017, 35, 281-289.	16.0	247
406	Single-Particle Tracking Reveals a Dynamic Role of Actin Filaments in Assisting Long-Range Axonal Transport in Neurons. Bulletin of the Chemical Society of Japan, 2017, 90, 714-719.	3.2	0
407	On the characteristics of airflow through the perforated tiles for raised-floor data centers. Journal of Building Engineering, 2017, 10, 60-68.	3.4	19
408	An assessment of emission event trends within the Greater Houston area during 2003–2013. Air Quality, Atmosphere and Health, 2017, 10, 543-554.	3.3	4
409	Epigenetic landscapes reveal transcription factors that regulate CD8+ T cell differentiation. Nature Immunology, 2017, 18, 573-582.	14.5	193
410	Reliable Förster Resonance Energy Transfer Probe Based on Structure-Switching DNA for Ratiometric Sensing of Telomerase in Living Cells. Analytical Chemistry, 2017, 89, 4216-4222.	6.5	82
411	Amyloid β induces NLRP3 inflammasome activation in retinal pigment epithelial cells via NADPH oxidase― and mitochondriaâ€dependent ROS production. Journal of Biochemical and Molecular Toxicology, 2017, 31, e21887.	3.0	53
412	Metal-free photosensitizers based on benzodithienothiophene as π-conjugated spacer for dye-sensitized solar cells. Organic Electronics, 2017, 42, 275-283.	2.6	16
413	New approach to morphological control for polypropylene/polyethylene blends via magnetic self-organization. Materials and Design, 2017, 117, 24-36.	7.0	21
414	Probing the Binding Interfaces of Histone-Aptamer by Photo Cross-Linking Mass Spectrometry. ACS Chemical Biology, 2017, 12, 57-62.	3.4	6

#	Article	IF	CITATIONS
415	Strategy for the detection of mercury ions by using exonuclease III-aided target recycling. RSC Advances, 2017, 7, 50420-50424.	3.6	12
416	Damping behaviors of granular particles in a vertically vibrated closed container. Powder Technology, 2017, 321, 173-179.	4.2	25
417	Polymer-Grafted Nanoparticle Membranes with Controllable Free Volume. Macromolecules, 2017, 50, 7111-7120.	4.8	88
418	Modelling study of the low-pump-power demand constructal T-shaped pipe network for a large scale radiative cooled-cold storage system. Applied Thermal Engineering, 2017, 127, 1564-1573.	6.0	22
419	Applications of Optobiology in Intact Cells and Multicellular Organisms. Journal of Molecular Biology, 2017, 429, 2999-3017.	4.2	27
420	Endogenous MicroRNA-Triggered and Real-Time Monitored Drug Release via Cascaded Energy Transfer Payloads. Analytical Chemistry, 2017, 89, 10239-10247.	6.5	19
421	Polarization-induced saw-tooth-like potential distribution in zincblende-wurtzite superlattice for efficient charge separation. Nano Energy, 2017, 41, 101-108.	16.0	53
422	Maleic Anhydride Labeling-Based Approach for Quantitative Proteomics and Successive Derivatization of Peptides. Analytical Chemistry, 2017, 89, 8259-8265.	6.5	9
423	Light-mediated Reversible Modulation of the Mitogen-activated Protein Kinase Pathway during Cell Differentiation and Xenopus Embryonic Development. Journal of Visualized Experiments, 2017, , .	0.3	5
424	Cobalt phosphide nanoparticles embedded in nitrogen-doped carbon nanosheets: Promising anode material with high rate capability and long cycle life for sodium-ion batteries. Nano Research, 2017, 10, 4337-4350.	10.4	97
425	Molecular Simulations of Solute Transport in Polymer Melts. ACS Macro Letters, 2017, 6, 864-868.	4.8	21
426	Efficient and provably secure identity-based multi-signature schemes for data aggregation in marine wireless sensor networks. , 2017, , .		4
427	Ultralow percolation threshold and enhanced electromagnetic interference shielding in poly(<scp>l</scp> -lactide)/multi-walled carbon nanotube nanocomposites with electrically conductive segregated networks. Journal of Materials Chemistry C, 2017, 5, 9359-9369.	5.5	322
428	Neuroprotective effect of tetramethylpyrazine against all-trans-retinal toxicity in the differentiated Y-79 cells via upregulation of IRBP expression. Experimental Cell Research, 2017, 359, 120-128.	2.6	12
429	Ultrasmall Superparamagnetic Iron Oxide Nanoparticle for <i>T</i> ₂ -Weighted Magnetic Resonance Imaging. ACS Applied Materials & Interfaces, 2017, 9, 28959-28966.	8.0	61
430	Sacrificial Interlayer for Promoting Charge Transport in Hematite Photoanode. ACS Applied Materials & Interfaces, 2017, 9, 42723-42733.	8.0	61
431	Finding a Needle in the Haystack: Identification of Functionally Important Minority Phases in an Operating Battery. Nano Letters, 2017, 17, 7782-7788.	9.1	42
432	Increasing Gas Bubble Escape Rate for Water Splitting with Nonwoven Stainless Steel Fabrics. ACS Applied Materials & Interfaces, 2017, 9, 40281-40289.	8.0	56

#	Article	IF	CITATIONS
433	Crystal structure of E. coli apolipoprotein N-acyl transferase. Nature Communications, 2017, 8, 15948.	12.8	31
434	Weather is not significantly correlated with destination-specific transport-related physical activity among adults: A large-scale temporally matched analysis. Preventive Medicine, 2017, 101, 133-136.	3.4	7
435	A new method for sensitive detection of microphthalmia-associated transcription factor based on "OFF-state―and "ON-state―equilibrium of a well-designed probe and duplex-specific nuclease signal amplification. Biosensors and Bioelectronics, 2017, 87, 299-304.	10.1	14
436	Sensitive detection of microRNA in complex biological samples by using two stages DSN-assisted target recycling signal amplification method. Biosensors and Bioelectronics, 2017, 87, 358-364.	10.1	78
437	Simultaneous Removal of Multiple DNA Segments by Polymerase Chain Reactions. Methods in Molecular Biology, 2017, 1472, 193-203.	0.9	1
438	Differences in environmental exposure assignment due to residential mobility among children with a central nervous system tumor: Texas, 1995–2009. Journal of Exposure Science and Environmental Epidemiology, 2017, 27, 41-46.	3.9	12
439	Reliable Robust Control for the System with Input Saturation Based on Gain Scheduling. Circuits, Systems, and Signal Processing, 2017, 36, 2586-2604.	2.0	4
440	Entropy-driven reactions in living cells for assay let-7a microRNA. Analytica Chimica Acta, 2017, 949, 53-58.	5.4	17
441	Robust H _{â^ž} dynamic output feedback control for spacecraft rendezvous with poles and input constraint. International Journal of Systems Science, 2017, 48, 1022-1034.	5.5	6
442	Air-conditioning system with underfloor air distribution integrated solar chimney in data center. Procedia Engineering, 2017, 205, 3420-3427.	1.2	3
443	Investigation of Adopting Shrink-Fit Multilayered Aluminum Shell in High-Field Common-Coil Accelerator Dipole Magnet. IEEE Transactions on Applied Superconductivity, 2017, 27, 1-4.	1.7	0
444	Electromagnetic design of a 12 T twin-aperture dipole magnet. International Journal of Modern Physics A, 2017, 32, 1746008.	1.5	13
445	Drive the Car(go)s—New Modalities to Control Cargo Trafficking in Live Cells. Frontiers in Molecular Neuroscience, 2017, 10, 4.	2.9	5
446	Scalable and Soundness Verifiable Outsourcing Computation in Marine Mobile Computing. Wireless Communications and Mobile Computing, 2017, 2017, 1-11.	1.2	4
447	Localization and diagnosis framework for pediatric cataracts based on slit-lamp images using deep features of a convolutional neural network. PLoS ONE, 2017, 12, e0168606.	2.5	72
448	Automatic diagnosis of imbalanced ophthalmic images using a cost-sensitive deep convolutional neural network. BioMedical Engineering OnLine, 2017, 16, 132.	2.7	36
449	PSDAAP: Provably Secure Data Authenticated Aggregation Protocols Using Identity-Based Multi-Signature in Marine WSNs. Sensors, 2017, 17, 2117.	3.8	5
450	Provably Secure Dual-Mode Publicly Verifiable Computation Protocol in Marine Wireless Sensor Networks. Lecture Notes in Computer Science, 2017, , 210-219.	1.3	3

#	Article	IF	CITATIONS
451	Runx3 programs CD8+ T cell residency in non-lymphoid tissues and tumours. Nature, 2017, 552, 253-257.	27.8	471
452	Neuroprotective Effect of Puerarin on Glutamate-Induced Cytotoxicity in Differentiated Y-79 Cells via Inhibition of ROS Generation and Ca2+ Influx. International Journal of Molecular Sciences, 2016, 17, 1109.	4.1	20
453	MicroRNAs as regulators of drug abuse and immunity. Central-European Journal of Immunology, 2016, 4, 426-434.	1.2	8
454	Public Health Impact and Economic Costs of Volkswagen's Lack of Compliance with the United States' Emission Standards. International Journal of Environmental Research and Public Health, 2016, 13, 891.	2.6	15
455	Ziyuglycoside I Inhibits the Proliferation of MDA-MB-231 Breast Carcinoma Cells through Inducing p53-Mediated G2/M Cell Cycle Arrest and Intrinsic/Extrinsic Apoptosis. International Journal of Molecular Sciences, 2016, 17, 1903.	4.1	25
456	A Preliminary Study on Sinus Fungus Ball with MicroCT and X-Ray Fluorescence Technique. PLoS ONE, 2016, 11, e0148515.	2.5	9
457	Preliminary research on dual-energy X-ray phase-contrast imaging. Chinese Physics C, 2016, 40, 048201.	3.7	6
458	MEDAPs: secure multi-entities delegated authentication protocols for mobile cloud computing. Security and Communication Networks, 2016, 9, 3777-3789.	1.5	16
459	Carbazole-based two-photon fluorescent probe for selective imaging of mitochondrial hydrogen peroxide in living cells and tissues. RSC Advances, 2016, 6, 115298-115302.	3.6	16
460	Disturbance observer-based sliding mode control for spacecraft non-cooperative rendezvous. , 2016, ,		6
461	New application of partitioning methodology: identityâ€based dual receiver encryption. Security and Communication Networks, 2016, 9, 5789-5802.	1.5	7
462	Constructing 3D interaction maps from 1D epigenomes. Nature Communications, 2016, 7, 10812.	12.8	135
463	Some properties of impossible differential and zero correlation linear cryptanalysis on TEA familyâ€ŧype ciphers. Security and Communication Networks, 2016, 9, 5746-5755.	1.5	1
464	Systematic identification of protein combinations mediating chromatin looping. Nature Communications, 2016, 7, 12249.	12.8	38
465	miR-181a is a negative regulator of GRIA2 in methamphetamine-use disorder. Scientific Reports, 2016, 6, 35691.	3.3	19
466	Sliding mode control based on robust parametric approach for spacecraft rendezvous. , 2016, , .		0
467	R&D steps of a 12-T common coil dipole magnet for SPPC pre-study. International Journal of Modern Physics A, 2016, 31, 1644018.	1.5	11
468	Mechanical Design of FECD1 at IHEP: a 12-T Hybrid Common-coil Dipole Magnet. IEEE Transactions on Applied Superconductivity, 2016, , 1-1.	1.7	4

#	Article	IF	CITATIONS
469	Galectin-1 knockdown in carcinoma-associated fibroblasts inhibits migration and invasion of human MDA-MB-231 breast cancer cells by modulating MMP-9 expression. Acta Biochimica Et Biophysica Sinica, 2016, 48, 462-467.	2.0	32
470	2-D Mechanical Design Study of a 20-T Two-in-One Common-Coil Dipole Magnet for High-Energy Accelerators. IEEE Transactions on Applied Superconductivity, 2016, 26, 1-5.	1.7	8
471	Gctf: Real-time CTF determination and correction. Journal of Structural Biology, 2016, 193, 1-12.	2.8	3,244
472	Nanooctahedra Particles Assembled FeSe ₂ Microspheres Embedded into Sulfur-Doped Reduced Graphene Oxide Sheets As a Promising Anode for Sodium Ion Batteries. ACS Applied Materials & Interfaces, 2016, 8, 13849-13856.	8.0	135
473	Spatiotemporal analysis of heat and heat wave effects on elderly mortality in Texas, 2006–2011. Science of the Total Environment, 2016, 562, 845-851.	8.0	42
474	Simplified model and submodule capacitor voltage balancing of singleâ€phase AC/AC modular multilevel converter for railway traction purpose. IET Power Electronics, 2016, 9, 951-959.	2.1	34
475	Formation of thermally conductive networks in isotactic polypropylene/hexagonal boron nitride composites via "Bridge Effect―of multi-wall carbon nanotubes and graphene nanoplatelets. RSC Advances, 2016, 6, 98571-98580.	3.6	29
476	Reversible optogenetic control of kinase activity during differentiation and embryonic development. Development (Cambridge), 2016, 143, 4085-4094.	2.5	48
477	Practical and Efficient Attribute-Based Encryption with Constant-Size Ciphertexts in Outsourced Verifiable Computation. , 2016, , .		13
478	Urchinâ€Like CoSe ₂ as a Highâ€Performance Anode Material for Sodiumâ€lon Batteries. Advanced Functional Materials, 2016, 26, 6728-6735.	14.9	471
479	Compensatory neural mechanisms in cognitively unimpaired <scp>P</scp> arkinson disease. Annals of Neurology, 2016, 79, 448-463.	5.3	62
480	Puerarin Protects Human Neuroblastoma SH‣Y5Y Cells against Glutamateâ€Induced Oxidative Stress and Mitochondrial Dysfunction. Journal of Biochemical and Molecular Toxicology, 2016, 30, 22-28.	3.0	25
481	FoxM1 inhibition enhances chemosensitivity of docetaxel-resistant A549 cells to docetaxel via activation of JNK/mitochondrial pathway. Acta Biochimica Et Biophysica Sinica, 2016, 48, 804-809.	2.0	26
482	Angular signal radiography. Optics Express, 2016, 24, 5829.	3.4	17
483	Cobaltâ€Doped FeS ₂ Nanospheres with Complete Solid Solubility as a Highâ€Performance Anode Material for Sodiumâ€Ion Batteries. Angewandte Chemie - International Edition, 2016, 55, 12822-12826.	13.8	394
484	Induction of oxidative and nitrosative stresses in human retinal pigment epithelial cells by all-trans-retinal. Experimental Cell Research, 2016, 348, 87-94.	2.6	24
485	Recent Developments of the Lithium Metal Anode for Rechargeable Nonâ€Aqueous Batteries. Advanced Energy Materials, 2016, 6, 1600811.	19.5	306
486	Control of the Crystalline Morphology of Poly(<scp>l</scp> -lactide) by Addition of High-Melting-Point Poly(<scp>l</scp> -lactide) and Its Effect on the Distribution of Multiwalled Carbon Nanotubes. Journal of Physical Chemistry B, 2016, 120, 7423-7437.	2.6	40

#	Article	IF	CITATIONS
487	Ubiquitin ligase RNF20/40 facilitates spindle assembly and promotes breast carcinogenesis through stabilizing motor protein Eg5. Nature Communications, 2016, 7, 12648.	12.8	50
488	Magnetic Responsive Polymer Nanocomposites with <i>In–situ</i> Tunable Anisotropy by Magnetic Selfâ€Organization. ChemistrySelect, 2016, 1, 5542-5546.	1.5	6
489	A label-free kissing complex-induced fluorescence sensor for DNA and RNA detection by using DNA-templated silver nanoclusters as a signal transducer. RSC Advances, 2016, 6, 99269-99273.	3.6	6
490	Short-term associations of fine particulate matter components and emergency hospital admissions among a privately insured population in Greater Houston. Atmospheric Environment, 2016, 147, 369-375.	4.1	19
491	Identification of hydroxylation at aromatic amino acid residues in yeast kinase using mass spectrometry with affinity enrichment. Rapid Communications in Mass Spectrometry, 2016, 30, 185-189.	1.5	2
492	Heat effects among migrant and seasonal farmworkers: a case study in Colorado. Occupational and Environmental Medicine, 2016, 73, 324-328.	2.8	9
493	Synchrotron radiation (SR) diffraction enhanced imaging (DEI) of chronic glomerulonephritis (CGN) mode. Journal of X-Ray Science and Technology, 2016, 24, 145-159.	1.0	1
494	Development of a DNAâ€Templated Peptide Probe for Photoaffinity Labeling and Enrichment of the Histone Modification Reader Proteins. Angewandte Chemie - International Edition, 2016, 55, 7993-7997.	13.8	29
495	Fine particulate matter components and emergency department visits among a privately insured population in Greater Houston. Science of the Total Environment, 2016, 566-567, 521-527.	8.0	20
496	FIRT: Filtered iterative reconstruction technique with information restoration. Journal of Structural Biology, 2016, 195, 49-61.	2.8	26
497	Experimental parametric study on the temperature distribution of an underfloor air distribution (UFAD) system with grille diffusers. Indoor and Built Environment, 2016, 25, 748-757.	2.8	5
498	Risks of developing breast and colorectal cancer in association with incomes and geographic locations in Texas: a retrospective cohort study. BMC Cancer, 2016, 16, 294.	2.6	22
499	Batch Verifiable Computation with Public Verifiability for Outsourcing Polynomials and Matrix Computations. Lecture Notes in Computer Science, 2016, , 293-309.	1.3	11
500	Facile synthesis and electrochemical sodium storage of CoS2 micro/nano-structures. Nano Research, 2016, 9, 198-206.	10.4	142
501	20-T Dipole Magnet With Common-Coil Configuration: Main Characteristics and Challenges. IEEE Transactions on Applied Superconductivity, 2016, 26, 1-4.	1.7	21
502	Rheology behavior and optimal damping effect of granular particles in a non-obstructive particle damper. Journal of Sound and Vibration, 2016, 364, 30-43.	3.9	60
503	Shear-induced orientation of functional graphene oxide sheets in isotactic polypropylene. Journal of Materials Science, 2016, 51, 5185-5195.	3.7	34
504	Brain-derived neurotrophic factor serum levels in heroin-dependent patients after 26weeks of withdrawal. Comprehensive Psychiatry, 2016, 65, 150-155.	3.1	30

#	Article	IF	CITATIONS
505	Investigation of Adopting Ti–15V–3Cr–3Sn–3Al Tie Rod to Support the Cold Mass of Superconducting Magnet With Strict Alignment Requirements. IEEE Transactions on Applied Superconductivity, 2016, 26, 1-6.	1.7	0
506	The Development of HTS Solenoid Lens for Electron Microscope. IEEE Transactions on Applied Superconductivity, 2016, 26, 1-6.	1.7	3
507	Sub-500  nm hard x ray focusing by compound long kinoform lenses. Applied Optics, 2016, 55, 38.	2.1	7
508	Maternal residential proximity to major roadways at delivery and childhood central nervous system tumors. Environmental Research, 2016, 146, 315-322.	7.5	16
509	Profiling post-translational modifications of histones in neural differentiation of embryonic stem cells using liquid chromatography–mass spectrometry. Journal of Chromatography B: Analytical Technologies in the Biomedical and Life Sciences, 2016, 1017-1018, 36-44.	2.3	5
510	A molecularly imprinted polymer as an antibody mimic with affinity for lysine acetylated peptides. Journal of Materials Chemistry B, 2016, 4, 920-928.	5.8	38
511	A label-free kissing complexes-induced fluorescence aptasensor using DNA-templated silver nanoclusters as a signal transducer. Biosensors and Bioelectronics, 2016, 78, 154-159.	10.1	28
512	Simplified model for desired airflow rate in underfloor air distribution (UFAD) systems. Applied Thermal Engineering, 2016, 93, 244-250.	6.0	21
513	A one-pot strategy for the sensitive detection of miRNA by catalyst–oligomer-mediated enzymatic amplification-based fluorescence biosensor. Sensors and Actuators B: Chemical, 2016, 223, 586-590.	7.8	14
514	Low-Frequency Ripple Suppression for Medium-Voltage Drives Using Modular Multilevel Converter With Full-Bridge Submodules. IEEE Journal of Emerging and Selected Topics in Power Electronics, 2016, 4, 657-667.	5.4	80
515	Sensitive detection of transcription factors in cell nuclear extracts by using a molecular beacons based amplification strategy. Biosensors and Bioelectronics, 2016, 77, 264-269.	10.1	26
516	Gas1 Knockdown Increases the Neuroprotective Effect of Glial Cell-Derived Neurotrophic Factor Against Glutamate-Induced Cell Injury in Human SH-SY5Y Neuroblastoma Cells. Cellular and Molecular Neurobiology, 2016, 36, 603-611.	3.3	9
517	Stabilization of histone demethylase PHF8 by USP7 promotes breast carcinogenesis. Journal of Clinical Investigation, 2016, 126, 2205-2220.	8.2	149
518	The Timing of Raf/ERK and AKT Activation in Protecting PC12 Cells against Oxidative Stress. PLoS ONE, 2016, 11, e0153487.	2.5	28
519	Zero Correlation Linear Cryptanalysis on LEA Family Ciphers. Journal of Communications, 2016, , .	1.6	2
520	Analytic signal extraction approach based on 2D Grating Interferometer and systematic comparison between 2D GI and 1D case. Journal of Instrumentation, 2016, 11, C03031-C03031.	1.2	0
521	Beyond packing of hard spheres: The effects of core softness, non-additivity, intermediate-range repulsion, and many-body interactions on the glass-forming ability of bulk metallic glasses. Journal of Chemical Physics, 2015, 143, 184502.	3.0	18
522	The glass-forming ability of model metal-metalloid alloys. Journal of Chemical Physics, 2015, 142, 104504.	3.0	15

#	Article	IF	CITATIONS
523	Trafficâ€related air pollution and the incidence of childhood central nervous system tumors: Texas, 2001–2009. Pediatric Blood and Cancer, 2015, 62, 1572-1578.	1.5	54
524	Recent Advances and Prospects of Cathode Materials for Sodiumâ€lon Batteries. Advanced Materials, 2015, 27, 5343-5364.	21.0	915
525	Ciliary neurotrophic factor protects SH-SY5Y neuroblastoma cells against AÎ ² 1-42 -induced neurotoxicity via activating the JAK2/STAT3 axis. Folia Neuropathologica, 2015, 3, 226-235.	1.2	19
526	Tetramethylpyrazine Protects Retinal Capillary Endothelial Cells (TR-iBRB2) against IL-1Î ² -Induced Nitrative/Oxidative Stress. International Journal of Molecular Sciences, 2015, 16, 21775-21790.	4.1	26
527	<p class="HeadingRunIn">The external and internal structures of Amphizoa davidi Lucas (Coleoptera, Amphizoidae), using X-ray phase contrast microtomography</p> . Zootaxa, 2015, 3963, 335.	0.5	3
528	High-performance sodium batteries with the 9,10-anthraquinone/CMK-3 cathode and an ether-based electrolyte. Chemical Communications, 2015, 51, 10244-10247.	4.1	117
529	Impact of the 2011 heat wave on mortality and emergency department visits in Houston, Texas. Environmental Health, 2015, 14, 11.	4.0	58
530	FeS ₂ microspheres with an ether-based electrolyte for high-performance rechargeable lithium batteries. Journal of Materials Chemistry A, 2015, 3, 12898-12904.	10.3	111
531	The Dual Characteristics of Light-Induced Cryptochrome 2, Homo-oligomerization and Heterodimerization, for Optogenetic Manipulation in Mammalian Cells. ACS Synthetic Biology, 2015, 4, 1124-1135.	3.8	57
532	Sn–Al core–shell nanocomposite as thin film anode for lithium-ion batteries. Journal of Alloys and Compounds, 2015, 644, 742-749.	5.5	17
533	Use of Synchrotron Radiation-Analytical Techniques To Reveal Chemical Origin of Silver-Nanoparticle Cytotoxicity. ACS Nano, 2015, 9, 6532-6547.	14.6	246
534	Retrograde NGF Axonal Transport—Motor Coordination in the Unidirectional Motility Regime. Biophysical Journal, 2015, 108, 2691-2703.	0.5	19
535	Tomographic observation of integrated circuit based on x-ray microscopy. , 2015, , .		1
536	U0126 Protects Cells against Oxidative Stress Independent of Its Function as a MEK Inhibitor. ACS Chemical Neuroscience, 2015, 6, 130-137.	3.5	41
537	Sulfur Nanodots Electrodeposited on Ni Foam as High-Performance Cathode for Li–S Batteries. Nano Letters, 2015, 15, 721-726.	9.1	175
538	Quantitative proteomics reveals the downregulation of GRB2 as a prominent node of F806-targeted cell proliferation network. Journal of Proteomics, 2015, 117, 145-155.	2.4	15
539	The structure of the dynactin complex and its interaction with dynein. Science, 2015, 347, 1441-1446.	12.6	389
540	Pyrite FeS ₂ for high-rate and long-life rechargeable sodium batteries. Energy and Environmental Science, 2015, 8, 1309-1316.	30.8	628

#	Article	IF	CITATIONS
541	Cold Mass Support Structure Design of MRI Superconducting Magnet Developed by IHEP. IEEE Transactions on Applied Superconductivity, 2015, 25, 1-6.	1.7	4
542	Magnetic Design Study of the High-Field Common-Coil Dipole Magnet for High-Energy Accelerators. IEEE Transactions on Applied Superconductivity, 2015, 25, 1-5.	1.7	19
543	Functional neuroimaging of acute oculomotor deficits in concussed athletes. Brain Imaging and Behavior, 2015, 9, 564-573.	2.1	64
544	A user-friendly nano-CT image alignment and 3D reconstruction platform based on LabVIEW. Chinese Physics C, 2015, 39, 018001.	3.7	12
545	Effect of cooling on the structure and electrochemical properties of 0.3Li2MnO3 · 0.7LiNi0.5Mn0.5O2 cathode material. Ionics, 2015, 21, 1819-1825.	2.4	6
546	Association between the efficacy of fluoxetine treatment in obsessive–compulsive disorder patients and SLC1A1 in a Han Chinese population. Psychiatry Research, 2015, 229, 631-632.	3.3	6
547	An Efficient and Secure Delegated Multi-authentication Protocol for Mobile Data Owners in Cloud. Lecture Notes in Computer Science, 2015, , 612-622.	1.3	4
548	The RhoGAP SPIN6 Associates with SPL11 and OsRac1 and Negatively Regulates Programmed Cell Death and Innate Immunity in Rice. PLoS Pathogens, 2015, 11, e1004629.	4.7	99
549	Determination of adsorption isotherm parameters with correlated errors by measurement error models. Chemical Engineering Journal, 2015, 281, 921-930.	12.7	29
550	Experimental research on the feature of an x-ray Talbot–Lau interferometer versus tube accelerating voltage. Chinese Physics B, 2015, 24, 068703.	1.4	6
551	Cosine fitting radiography and computed tomography. Chinese Physics B, 2015, 24, 068704.	1.4	2
552	Multiplex gene removal by two-step polymerase chain reactions. Analytical Biochemistry, 2015, 481, 7-9.	2.4	4
553	A novel crystal-analyzer phase retrieval algorithm and its noise property. Journal of Synchrotron Radiation, 2015, 22, 786-795.	2.4	6
554	An assessment of air pollutant exposure methods in Mexico City, Mexico. Journal of the Air and Waste Management Association, 2015, 65, 581-591.	1.9	51
555	FeSe ₂ Microspheres as a Highâ€Performance Anode Material for Naâ€lon Batteries. Advanced Materials, 2015, 27, 3305-3309.	21.0	581
556	Highâ€Performance Organic Lithium Batteries with an Etherâ€Based Electrolyte and 9,10â€Anthraquinone (AQ)/CMKâ€3 Cathode. Advanced Science, 2015, 2, 1500018.	11.2	155
557	Quantitative characterization of histone post-translational modifications using a stable isotope dimethyl-labeling strategy. Analytical Methods, 2015, 7, 3779-3785.	2.7	4
558	Optogenetic Control of Molecular Motors and Organelle Distributions in Cells. Chemistry and Biology, 2015, 22, 671-682.	6.0	88

#	Article	IF	CITATIONS
559	High sensitivity phase retrieval method in gratingâ€based xâ€ray phase contrast imaging. Medical Physics, 2015, 42, 741-749.	3.0	18
560	On the origin of multi-component bulk metallic glasses: Atomic size mismatches and de-mixing. Journal of Chemical Physics, 2015, 143, 054501.	3.0	25
561	Novel dialkoxy-substituted benzodithienothiophenes for high-performance organic field-effect transistors. Journal of Materials Chemistry C, 2015, 3, 10892-10897.	5.5	6
562	Click Synthesis of Hydrophilic Maltose-Functionalized Iron Oxide Magnetic Nanoparticles Based on Dopamine Anchors for Highly Selective Enrichment of Glycopeptides. ACS Applied Materials & Interfaces, 2015, 7, 24670-24678.	8.0	92
563	A new signal-on method for the detection of protein based on binding-induced strategy and photoinduced electron transfer between Ag nanoclusters and split G-quadruplex-hemin complexes. Analytica Chimica Acta, 2015, 887, 224-229.	5.4	11
564	Analytical strategies used to identify the readers of histone modifications: A review. Analytica Chimica Acta, 2015, 891, 32-42.	5.4	11
565	Indirect vector control with simplified rotor resistance adaptation for induction machines. IET Power Electronics, 2015, 8, 1284-1294.	2.1	42
566	Identification of Two Novel Modifications at Tryptophan Residues. Journal of the American Society for Mass Spectrometry, 2015, 26, 1787-1790.	2.8	1
567	Fine particulate matter components and mortality in Greater Houston: Did the risk reduce from 2000 to 2011?. Science of the Total Environment, 2015, 538, 162-168.	8.0	32
568	Daily Estimation of Ground-Level PM _{2.5} Concentrations over Beijing Using 3 km Resolution MODIS AOD. Environmental Science & Technology, 2015, 49, 12280-12288.	10.0	240
569	Soil as an inexhaustible and high-performance anode material for Li-ion batteries. Chemical Communications, 2015, 51, 15827-15830.	4.1	6
570	Polymerase chain reaction-based gene removal from plasmids. Data in Brief, 2015, 4, 75-82.	1.0	4
571	Sensitive and selective amplified detection of silver ion based on NEase-aided target recycling. RSC Advances, 2015, 5, 89047-89051.	3.6	4
572	Improved conditional differential cryptanalysis. Security and Communication Networks, 2015, 8, 1801-1811.	1.5	5
573	Optogenetic control of intracellular signaling pathways. Trends in Biotechnology, 2015, 33, 92-100.	9.3	208
574	An Improved Control System for Modular Multilevel Converters with New Modulation Strategy and Voltage Balancing Control. IEEE Transactions on Power Electronics, 2015, 30, 358-371.	7.9	168
575	A Repetitive Control Scheme for Harmonic Suppression of Circulating Current in Modular Multilevel Converters. IEEE Transactions on Power Electronics, 2015, 30, 471-481.	7.9	192
576	Nanostructured Mn-based oxides for electrochemical energy storage and conversion. Chemical Society Reviews, 2015, 44, 699-728.	38.1	740

#	Article	IF	CITATIONS
577	Binding-induced and label-free colorimetric method for protein detection based on autonomous assembly of hemin/G-quadruplex DNAzyme amplification strategy. Biosensors and Bioelectronics, 2015, 64, 572-578.	10.1	52
578	Comparative analysis of histone H3 and H4 post-translational modifications of esophageal squamous cell carcinoma with different invasive capabilities. Journal of Proteomics, 2015, 112, 180-189.	2.4	33
579	Visualizing Directional Rab7 and TrkA Cotrafficking in Axons by pTIRF Microscopy. Methods in Molecular Biology, 2015, 1298, 319-329.	0.9	7
580	A Modified Capacitor Current Feedback Active Damping Approach for Grid Connected Converters with an LCL Filter. Journal of Power Electronics, 2015, 15, 1286-1294.	1.5	4
581	Original article Neuroprotective properties of ciliary neurotrophic factor on retinoic acid (RA)-predifferentiated SH-SY5Y neuroblastoma cells. Folia Neuropathologica, 2014, 2, 121-127.	1.2	8
582	DEIReconstructor: a software for diffraction enhanced imaging processing and tomography reconstruction. Chinese Physics C, 2014, 38, 106202.	3.7	2
583	Inorganic & organic materials for rechargeable Li batteries with multi-electron reaction. Science China Materials, 2014, 57, 42-58.	6.3	78
584	Development of an Eddy-current Separation Equipment with High gradient Superconducting Magnet. IEEE Transactions on Applied Superconductivity, 2014, , 1-1.	1.7	3
585	Rational design of signal-on biosensors by using photoinduced electron transfer between Ag nanoclusters and split G-quadruplex halves–hemin complexes. Chemical Communications, 2014, 50, 14221-14224.	4.1	35
586	Using Forecast and Observed Weather Data to Assess Performance of Forecast Products in Identifying Heat Waves and Estimating Heat Wave Effects on Mortality. Environmental Health Perspectives, 2014, 122, 912-918.	6.0	27
587	Characterizing Spatial Patterns of Airborne Coarse Particulate (PM _{10–2.5}) Mass and Chemical Components in Three Cities: The Multi-Ethnic Study of Atherosclerosis. Environmental Health Perspectives, 2014, 122, 823-830.	6.0	29
588	Improved variable EWMA controller design. , 2014, , .		0
589	Potassium–Sulfur Batteries: A New Member of Room-Temperature Rechargeable Metal–Sulfur Batteries. Inorganic Chemistry, 2014, 53, 9000-9005.	4.0	163
590	Investigation of Gallic Acid Induced Anticancer Effect in Human Breast Carcinoma MCFâ€7 Cells. Journal of Biochemical and Molecular Toxicology, 2014, 28, 387-393.	3.0	81
591	An analysis and performance assessment of double EWMA control systems. , 2014, , .		0
592	Experimental study on the characteristics of supply air for UFAD system with perforated tiles. Energy and Buildings, 2014, 80, 1-6.	6.7	29
593	High level soluble expression, purification, and characterization of human ciliary neuronotrophic factor in Escherichia coli by single protein production system. Protein Expression and Purification, 2014, 96, 8-13.	1.3	4
594	Signal-to-noise ratio analysis of X-ray grating interferometry with the reverse projection extraction method. Journal of Electron Spectroscopy and Related Phenomena, 2014, 196, 75-79.	1.7	5

#	Article	IF	CITATIONS
595	Numerical Study on the Thermal Environment of UFAD System with Solar Chimney for the Data Center. Energy Procedia, 2014, 48, 1047-1054.	1.8	15
596	Protective Effect of Paeoniflorin on Aβ25–35-Induced SH-SY5Y Cell Injury by Preventing Mitochondrial Dysfunction. Cellular and Molecular Neurobiology, 2014, 34, 227-234.	3.3	90
597	Porous CuO nanowires as the anode of rechargeable Na-ion batteries. Nano Research, 2014, 7, 199-208.	10.4	233
598	MoS ₂ Nanoflowers with Expanded Interlayers as Highâ€Performance Anodes for Sodiumâ€lon Batteries. Angewandte Chemie - International Edition, 2014, 53, 12794-12798.	13.8	670
599	Preparation and characterization of vorinostat-coated beads for profiling of novel target proteins. Journal of Chromatography A, 2014, 1372, 34-41.	3.7	6
600	miR-200b suppresses invasiveness and modulates the cytoskeletal and adhesive machinery in esophageal squamous cell carcinoma cells via targeting Kindlin-2. Carcinogenesis, 2014, 35, 292-301.	2.8	53
601	Sensitive and selective amplified visual detection of cytokines based on exonuclease III-aided target recycling. Chemical Communications, 2014, 50, 13342-13345.	4.1	29
602	A PH Domain in ACAP1 Possesses Key Features of the BAR Domain in Promoting Membrane Curvature. Developmental Cell, 2014, 31, 73-86.	7.0	32
603	Uniformity Aspects of Superconducting MRI Magnet Developed by IHEP. IEEE Transactions on Applied Superconductivity, 2014, 24, 30-34.	1.7	0
604	Review of underfloor air distribution technology. Energy and Buildings, 2014, 85, 180-186.	6.7	47
605	High-Performance Indirect Current Control Scheme for Railway Traction Four-Quadrant Converters. IEEE Transactions on Industrial Electronics, 2014, 61, 6645-6654.	7.9	43
606	Na ₃ V ₂ (PO ₄) ₃ @C core–shell nanocomposites for rechargeable sodium-ion batteries. Journal of Materials Chemistry A, 2014, 2, 8668-8675.	10.3	348
607	Label-free and ultrasensitive fluorescence detection of cocaine based on a strategy that utilizes DNA-templated silver nanoclusters and the nicking endonuclease-assisted signal amplification method. Chemical Communications, 2014, 50, 180-182.	4.1	61
608	The 2011 heat wave in Greater Houston: Effects of land use on temperature. Environmental Research, 2014, 135, 81-87.	7.5	25
609	Broad-Spectrum Antiviral Property of Polyoxometalate Localized on a Cell Surface. ACS Applied Materials & Interfaces, 2014, 6, 9785-9789.	8.0	52
610	Lighting up FGFR Signaling. Chemistry and Biology, 2014, 21, 806-808.	6.0	1
611	Polypyrrole-cobalt-carbon nanocomposites as efficient counter electrode materials for dye-sensitized solar cells. Science China Chemistry, 2014, 57, 1559-1563.	8.2	7
612	Ziyuglycoside II induces cell cycle arrest and apoptosis through activation of ROS/JNK pathway in human breast cancer cells. Toxicology Letters, 2014, 227, 65-73.	0.8	62

#	Article	IF	CITATIONS
613	A general strategy based on luminescent oxygen channeling for the detection of adenosine in serum using the steric hindrance effect of thrombin. Sensors and Actuators B: Chemical, 2014, 200, 19-24.	7.8	2
614	What weather variables are important in predicting heat-related mortality? A new application of statistical learning methods. Environmental Research, 2014, 132, 350-359.	7.5	94
615	Ultrasensitive detection of microRNA with isothermal amplification and a time-resolved fluorescence sensor. Biosensors and Bioelectronics, 2014, 57, 91-95.	10.1	35
616	DNA-templated silver nanoclusters based label-free fluorescent molecular beacon for the detection of adenosine deaminase. Biosensors and Bioelectronics, 2014, 52, 124-128.	10.1	36
617	Cryo-EM structures of two bovine adenovirus type 3 intermediates. Virology, 2014, 450-451, 174-181.	2.4	31
618	C-terminal motif within Sec7 domain regulates guanine nucleotide exchange activity via tuning protein conformation. Biochemical and Biophysical Research Communications, 2014, 446, 380-386.	2.1	1
619	Hydrothermal synthesis of spindle-like Li2FeSiO4-C composite as cathode materials for lithium-ion batteries. Journal of Energy Chemistry, 2014, 23, 274-281.	12.9	19
620	Ultrasmall Li2S Nanoparticles Anchored in Graphene Nanosheets for High-Energy Lithium-Ion Batteries. Scientific Reports, 2014, 4, 6467.	3.3	122
621	Light-Mediated Kinetic Control Reveals the Temporal Effect of the Raf/MEK/ERK Pathway in PC12 Cell Neurite Outgrowth. PLoS ONE, 2014, 9, e92917.	2.5	94
622	Comprehensive Analysis for Histone Acetylation of Human Colon Cancer Cells Treated with a novel HDAC Inhibitor. Current Pharmaceutical Design, 2014, 20, 1866-1873.	1.9	19
623	Flexible interwoven termini determine the thermal stability of thermosomes. Protein and Cell, 2013, 4, 432-444.	11.0	13
624	A new method for the detection of adenosine based on time-resolved fluorescence sensor. Biosensors and Bioelectronics, 2013, 49, 226-230.	10.1	14
625	Li3V2(PO4)3@C core–shell nanocomposite as a superior cathode material for lithium-ion batteries. Nanoscale, 2013, 5, 6485.	5.6	130
626	Air pollution and health risks due to vehicle traffic. Science of the Total Environment, 2013, 450-451, 307-316.	8.0	457
627	Ziyuglycoside II Inhibits the Growth of Human Breast Carcinoma MDA-MB-435 Cells via Cell Cycle Arrest and Induction of Apoptosis through the Mitochondria Dependent Pathway. International Journal of Molecular Sciences, 2013, 14, 18041-18055.	4.1	43
628	Organic Li ₄ C ₈ H ₂ O ₆ Nanosheets for Lithium-Ion Batteries. Nano Letters, 2013, 13, 4404-4409.	9.1	352
629	Synthesis of CdS/CNTs photocatalysts and study of hydrogen production by photocatalytic water splitting. International Journal of Hydrogen Energy, 2013, 38, 13091-13096.	7.1	49
630	Identification of SERPINB1 As a Physiological Inhibitor of Human Granzyme H. Journal of Immunology, 2013, 190, 1319-1330.	0.8	31

#	Article	IF	CITATIONS
631	Repetitive control scheme for circulating current suppression in modular multilevel converters. , 2013, , .		3
632	Li2MnSiO4@C nanocomposite as a high-capacity cathode material for Li-ion batteries. Journal of Materials Chemistry A, 2013, 1, 12650.	10.3	41
633	Active Power Decoupling for High-Power Single-Phase PWM Rectifiers. IEEE Transactions on Power Electronics, 2013, 28, 1308-1319.	7.9	382
634	An enzyme substrate binding aptamer complex based time-resolved fluorescence sensor for the adenosine deaminasedetection. Biosensors and Bioelectronics, 2013, 42, 87-92.	10.1	19
635	Structural Insights into the Intrinsic Self-Assembly of Par-3 N-Terminal Domain. Structure, 2013, 21, 997-1006.	3.3	34
636	Composite of sulfur impregnated in porous hollow carbon spheres as the cathode of Li-S batteries with high performance. Nano Research, 2013, 6, 38-46.	10.4	232
637	Comprehensive Profiling of Protein Lysine Acetylation in <i>Escherichia coli</i> . Journal of Proteome Research, 2013, 12, 844-851.	3.7	234
638	Intergrown Li2FeSiO4·LiFePO4–C nanocomposites as high-capacity cathode materials for lithium-ion batteries. Chemical Communications, 2013, 49, 3040.	4.1	73
639	Protein lysine acetylation analysis: current MS-based proteomic technologies. Analyst, The, 2013, 138, 1628.	3.5	34
640	A new method to retrieve phase information for equiangular fan beam differential phase contrast computed tomography. Medical Physics, 2013, 40, 031911.	3.0	20
641	Atomic Model of Rabbit Hemorrhagic Disease Virus by Cryo-Electron Microscopy and Crystallography. PLoS Pathogens, 2013, 9, e1003132.	4.7	94
642	Metal sulphide semiconductors for photocatalytic hydrogen production. Catalysis Science and Technology, 2013, 3, 1672.	4.1	477
643	Temporary ileostomy versus colostomy for colorectal anastomosis: evidence from 12 studies. Scandinavian Journal of Gastroenterology, 2013, 48, 556-562.	1.5	29
644	TiO ₂ Single Crystal with Fourâ€Truncatedâ€Bipyramid Morphology as an Efficient Photocatalyst for Hydrogen Production. Small, 2013, 9, 2452-2459.	10.0	50
645	Functional porous carbon-based composite electrode materials for lithium secondary batteries. Journal of Energy Chemistry, 2013, 22, 214-225.	12.9	51
646	A new strategy based on aptasensor to time-resolved fluorescence assay for adenosine deaminase activity. Biosensors and Bioelectronics, 2013, 41, 123-128.	10.1	20
647	Scattering imaging method in transmission x-ray microscopy. Optics Letters, 2013, 38, 2068.	3.3	2
648	Validating Satellite-Derived Land Surface Temperature with <i>in Situ</i> Measurements: A Public Health Perspective. Environmental Health Perspectives, 2013, 121, 925-931.	6.0	59

#	Article	IF	CITATIONS
649	X-ray phase radiography and tomography with grating interferometry and the reverse projection technique. Journal Physics D: Applied Physics, 2013, 46, 494003.	2.8	11
650	Penetrating view of nano-structures inAleochara vernaspermatheca and flagellum by hard X-ray microscopy. Chinese Physics B, 2013, 22, 076801.	1.4	7
651	Chromatin-to-nucleoprotamine transition is controlled by the histone H2B variant TH2B. Genes and Development, 2013, 27, 1680-1692.	5.9	186
652	A Photoelectrochemical Investigation on the Synergetic Effect between CdS and Reduced Graphene Oxide for Solarâ€Energy Conversion. Chemistry - an Asian Journal, 2013, 8, 2395-2400.	3.3	45
653	Defective Axonal Transport of Rab7 GTPase Results in Dysregulated Trophic Signaling. Journal of Neuroscience, 2013, 33, 7451-7462.	3.6	88
654	Structure Reveals Regulatory Mechanisms of a MaoC-Like Hydratase from Phytophthora capsici Involved in Biosynthesis of Polyhydroxyalkanoates (PHAs). PLoS ONE, 2013, 8, e80024.	2.5	10
655	A Simple Spatial Working Memory and Attention Test on Paired Symbols Shows Developmental Deficits in Schizophrenia Patients. Neural Plasticity, 2013, 2013, 1-7.	2.2	4
656	Spindle-Like LiMnPO ₄ Assembled by Nanorods with Different Crystallographic Orientations as the Cathode of Lithium-Ion Batteries. Science of Advanced Materials, 2013, 5, 1676-1685.	0.7	6
657	Clinicopathological and prognostic significance of galectin-1 and vascular endothelial growth factor expression in gastric cancer. World Journal of Gastroenterology, 2013, 19, 2073.	3.3	47
658	An Investigation into the Spatial Variability of Near-Surface Air Temperatures in the Detroit, Michigan, Metropolitan Region. Journal of Applied Meteorology and Climatology, 2012, 51, 1290-1304.	1.5	30
659	Reconstructing a complex field from a series of its near-field diffraction patterns. Chinese Physics B, 2012, 21, 104202.	1.4	9
660	Extended depth of focus for transmission x-ray microscope. Optics Letters, 2012, 37, 3708.	3.3	33
661	Development of a 6-T Conduction-Cooled Superconducting Magnet. IEEE Transactions on Applied Superconductivity, 2012, 22, 4905605-4905605.	1.7	0
662	The Use of Magnetic Resonance Spectroscopy in the Subacute Evaluation of Athletes Recovering from Single and Multiple Mild Traumatic Brain Injury. Journal of Neurotrauma, 2012, 29, 2297-2304.	3.4	63
663	Default Mode Network in Concussed Individuals in Response to the YMCA Physical Stress Test. Journal of Neurotrauma, 2012, 29, 756-765.	3.4	70
664	A novel active power decoupling method for single-phase photovoltaic or energy storage applications. , 2012, , .		38
665	Mechanistic Insights into Regulated Cargo Binding by ACAP1 Protein. Journal of Biological Chemistry, 2012, 287, 28675-28685.	3.4	25
666	Structural Insights into the Substrate Specificity of Human Granzyme H: The Functional Roles of a Novel RKR Motif. Journal of Immunology, 2012, 188, 765-773.	0.8	19

#	Article	IF	CITATIONS
667	A modified single-phase h-bridge PWM rectifier with power decoupling. , 2012, , .		11
668	Transient-free method of indirect current control for railway traction four-quadrant converters. , 2012, , .		1
669	Facile polymer-assisted synthesis of LiNi0.5Mn1.5O4 with a hierarchical micro–nano structure and high rate capability. RSC Advances, 2012, 2, 5669.	3.6	111
670	A thermally and electrochemically stable organic hole-transporting material with an adamantane central core and triarylamine moieties. Synthetic Metals, 2012, 162, 490-496.	3.9	47
671	Metabolic alterations in corpus callosum may compromise brain functional connectivity in MTBI patients: An 1H-MRS study. Neuroscience Letters, 2012, 509, 5-8.	2.1	45
672	Comparing exposure metrics for classifying â€~dangerous heat' in heat wave and health warning systems. Environment International, 2012, 46, 23-29.	10.0	61
673	Preparation and characterization of DNA aptamer based spin column for enrichment and separation of histones. Chemical Communications, 2012, 48, 6684.	4.1	17
674	A 30â€nm-resolution hard X-ray microscope with X-ray fluorescence mapping capability at BSRF. Journal of Synchrotron Radiation, 2012, 19, 1021-1028.	2.4	81
675	Alteration of brain default network in subacute phase of injury in concussed individuals: Resting-state fMRI study. NeuroImage, 2012, 59, 511-518.	4.2	268
676	Use of fractal zone plates for transmission X-ray microscopy. Analytical and Bioanalytical Chemistry, 2012, 404, 1303-1309.	3.7	8
677	High-speed X-ray microscopy by use of high-resolution zone plates and synchrotron radiation. Analytical and Bioanalytical Chemistry, 2012, 404, 1327-1330.	3.7	2
678	Functional characterization and axonal transport of quantum dot labeled BDNF. Integrative Biology (United Kingdom), 2012, 4, 953.	1.3	29
679	Cryo-EM structure of a transcribing cypovirus. Proceedings of the National Academy of Sciences of the United States of America, 2012, 109, 6118-6123.	7.1	52
680	Concussion in athletics: ongoing clinical and brain imaging research controversies. Brain Imaging and Behavior, 2012, 6, 224-243.	2.1	99
681	Extended hybrid pressure and velocity boundary conditions for D3Q27 lattice Boltzmann model. Applied Mathematical Modelling, 2012, 36, 2031-2055.	4.2	10
682	Porosity and permeability evolution and evaluation in anisotropic porosity multiscale-multiphase-multicomponent structure. Science Bulletin, 2012, 57, 320-327.	1.7	10
683	DC-Link Active Power Filter for High-Power Single-Phase PWM Converters. Journal of Power Electronics, 2012, 12, 458-467.	1.5	31
684	Real Time Related Key Attack on Hummingbird-2. KSII Transactions on Internet and Information Systems, 2012, , .	0.3	3

#	Article	IF	CITATIONS
685	Current separative strategies used for resveratrol determination from natural sources. Analytical Methods, 2011, 3, 2454.	2.7	17
686	Geostatistical exploration of spatial variation of summertime temperatures in the Detroit metropolitan region. Environmental Research, 2011, 111, 1046-1053.	7.5	42
687	Acetylation of ECF receptor contributes to tumor cell resistance to histone deacetylase inhibitors. Biochemical and Biophysical Research Communications, 2011, 404, 68-73.	2.1	39
688	Three-dimensional reconstruction using an adaptive simultaneous algebraic reconstruction technique in electron tomography. Journal of Structural Biology, 2011, 175, 277-287.	2.8	43
689	Isolation and functional characterization of P-TEFb-associated factors that control general and HIV-1 transcriptional elongation. Methods, 2011, 53, 85-90.	3.8	10
690	Repetitive Compensation of Fluctuating DC Link Voltage for Railway Traction Drives. IEEE Transactions on Power Electronics, 2011, 26, 2160-2171.	7.9	65
691	Autotransporter passenger domain secretion requires a hydrophobic cavity at the extracellular entrance of the Î ² -domain pore. Biochemical Journal, 2011, 435, 577-587.	3.7	39
692	Alkaline earth metal as a novel dopant for chalcogenide solid solution: Improvement of photocatalytic efficiency of Cd1â^xZnxS by barium surface doping. International Journal of Hydrogen Energy, 2011, 36, 9469-9478.	7.1	49
693	Vehicle emissions in congestion: Comparison of work zone, rush hour and free-flow conditions. Atmospheric Environment, 2011, 45, 1929-1939.	4.1	136
694	Active DC-link power filter for single phase PWM rectifiers. , 2011, , .		24
695	Study of OSEM with different subsets in grating-based X-ray differential phase-contrast imaging. Analytical and Bioanalytical Chemistry, 2011, 401, 837-844.	3.7	9
696	3D configuration of mandibles and controlling muscles in rove beetles based on micro-CT technique. Analytical and Bioanalytical Chemistry, 2011, 401, 817-825.	3.7	37
697	Investigation of the partially coherent effects in a 2D Talbot interferometer. Analytical and Bioanalytical Chemistry, 2011, 401, 865-870.	3.7	10
698	Application of flow driven pore-network crack model to Zipingpu reservoir and Longmenshan slip. Science China: Physics, Mechanics and Astronomy, 2011, 54, 1532-1540.	5.1	6
699	Automated image analysis for tracking cargo transport in axons. Microscopy Research and Technique, 2011, 74, 605-613.	2.2	28
700	Systematic screening of protein modifications in four kinases using affinity enrichment and mass spectrometry analysis with unrestrictive sequence alignment. Analytica Chimica Acta, 2011, 691, 62-67.	5.4	0
701	Grating-based X-ray phase contrast imaging using polychromatic laboratory sources. Journal of Electron Spectroscopy and Related Phenomena, 2011, 184, 342-345.	1.7	5

#	Article	IF	CITATIONS
703	Atomic model of a cypovirus built from cryo-EM structure provides insight into the mechanism of mRNA capping. Proceedings of the National Academy of Sciences of the United States of America, 2011, 108, 1373-1378.	7.1	65
704	Crystal Structure of a Novel Esterase Rv0045c from Mycobacterium tuberculosis. PLoS ONE, 2011, 6, e20506.	2.5	20
705	Substrate Binding Properties of Thermosome ATcpnβFrom <i>Acidianus Tengchongensis</i> . Progress in Biochemistry and Biophysics, 2011, 38, 151-158.	0.3	1
706	ATOM 1.0: A GPU Powered Package for Electron Tomography Reconstruction. Sheng Wu Wu Li Hsueh Bao, 2011, 27, 231-241.	0.1	1
707	Obtaining Resveratrol: from Chemical Synthesis to Biotechnological Production. Mini-Reviews in Organic Chemistry, 2010, 7, 272-281.	1.3	34
708	Tau Reduction Prevents AÎ ² -Induced Defects in Axonal Transport. Science, 2010, 330, 198-198.	12.6	436
709	Strategy to Fabricate an Electrochemical Aptasensor: Application to the Assay of Adenosine Deaminase Activity. Analytical Chemistry, 2010, 82, 3207-3211.	6.5	68
710	Quantitative coherence analysis with an X-ray Talbot–Lau interferometer. Analytical and Bioanalytical Chemistry, 2010, 397, 2091-2094.	3.7	21
711	Analysis of polychromaticity effects in X-ray Talbot interferometer. Analytical and Bioanalytical Chemistry, 2010, 397, 2137-2141.	3.7	26
712	Progress of diffraction enhanced imaging at the Beijing Synchrotron Radiation Facility. Analytical and Bioanalytical Chemistry, 2010, 397, 2067-2078.	3.7	6
713	3D visualization of the microstructure of Quedius beesoni Cameron using micro-CT. Analytical and Bioanalytical Chemistry, 2010, 397, 2143-2148.	3.7	17
714	Crystal Structure of Group II Chaperonin in the Open State. Structure, 2010, 18, 1270-1279.	3.3	38
715	Near-road air pollutant concentrations of CO and PM2.5: A comparison of MOBILE6.2/CALINE4 and generalized additive models. Atmospheric Environment, 2010, 44, 1740-1748.	4.1	53
716	Influence of Sr-doping on the photocatalytic activities of CdS–ZnS solid solution photocatalysts. International Journal of Hydrogen Energy, 2010, 35, 2048-2057.	7.1	123
717	SrS/CdS composite powder as a novel photocatalyst for hydrogen production under visible light irradiation. International Journal of Hydrogen Energy, 2010, 35, 7080-7086.	7.1	39
718	Efficient solar hydrogen production by photocatalytic water splitting: From fundamental study to pilot demonstration. International Journal of Hydrogen Energy, 2010, 35, 7087-7097.	7.1	273
719	Analysis of partial coherence in grating-based phase-contrast X-ray imaging. Nuclear Instruments and Methods in Physics Research, Section A: Accelerators, Spectrometers, Detectors and Associated Equipment, 2010, 619, 319-322.	1.6	7
720	New Developments of Quantitative Mass Spectrometry-based Proteomics. Chinese Journal of Analytical Chemistry, 2010, 38, 434-441.	1.7	5

#	Article	IF	CITATIONS
721	Unrestrictive identification of nonâ€phosphorylation PTMs in yeast kinases by MS and PTMap. Proteomics, 2010, 10, 896-903.	2.2	8
722	Low-dose, simple, and fast grating-based X-ray phase-contrast imaging. Proceedings of the National Academy of Sciences of the United States of America, 2010, 107, 13576-13581.	7.1	208
723	Single-molecule imaging of NGF axonal transport in microfluidic devices. Lab on A Chip, 2010, 10, 2566.	6.0	63
724	Prediction and analysis of near-road concentrations using a reduced-form emission/dispersion model. Environmental Health, 2010, 9, 29.	4.0	29
725	Five mutations in N-terminus confer thermostability on mesophilic xylanase. Biochemical and Biophysical Research Communications, 2010, 395, 200-206.	2.1	59
726	A novel indirect current control for single-phase PWM rectifier at low switching frequency. , 2010, , .		4
727	Optimizing Traffic Control to Reduce Fuel Consumption and Vehicular Emissions. Transportation Research Record, 2009, 2128, 105-113.	1.9	156
728	Bipolar cellular morphology of malignant melanoma in unstained human melanoma skin tissue. Journal of Biomedical Optics, 2009, 14, 024042.	2.6	3
729	Time allocation shifts and pollutant exposure due to traffic congestion: An analysis using the national human activity pattern survey. Science of the Total Environment, 2009, 407, 5493-5500.	8.0	20
730	Optically Resolving Individual Microtubules in Live Axons. Structure, 2009, 17, 1433-1441.	3.3	41
731	Identification and Verification of Lysine Propionylation and Butyrylation in Yeast Core Histones Using PTMap Software. Journal of Proteome Research, 2009, 8, 900-906.	3.7	141
732	D Structural Investigation of Caveolae From Porcine Aorta Endothelial Cell by Electron Tomography*. Progress in Biochemistry and Biophysics, 2009, 2009, 729-735.	0.3	3
733	Restrained ion population transfer: a novel ion transfer method for mass spectrometry. Rapid Communications in Mass Spectrometry, 2008, 22, 1955-1964.	1.5	9
734	Identification and Validation of Eukaryotic Aspartate and Glutamate Methylation in Proteins. Journal of Proteome Research, 2008, 7, 1001-1006.	3.7	65
735	Phase retrieval from a single near-field diffraction pattern with a large Fresnel number. Journal of the Optical Society of America A: Optics and Image Science, and Vision, 2008, 25, 2651.	1.5	7
736	Investigation of misalignment in analyzer crystal based-CT and its effect. Physics in Medicine and Biology, 2008, 53, 5757-5766.	3.0	5
737	Analysis of trans-Resveratrol in Grapes by Micro-High Performance Liquid Chromatography. Analytical Sciences, 2008, 24, 1019-1023.	1.6	11
738	Digital Active Common Mode EMI Suppression Technique for Switching Converters. , 2007, , .		4

#	Article	IF	CITATIONS
739	A new method to extract angle of refraction in diffraction enhanced imaging computed tomography. Journal Physics D: Applied Physics, 2007, 40, 6917-6921.	2.8	16
740	Single Quantum Dots as Local Temperature Markers. Nano Letters, 2007, 7, 3102-3105.	9.1	215
741	Continuous Distribution of Emission States from Single CdSe/ZnS Quantum Dots. Nano Letters, 2006, 6, 843-847.	9.1	228
742	Improved Dual-loop Control plus Repetitive Control for PWM Inverters. , 2006, , .		3
743	Three-Dimensional Chiral Imaging by Sum-Frequency Generation. Journal of the American Chemical Society, 2006, 128, 3482-3483.	13.7	56
744	Reduction of Common Mode EMI in a PWM Inverter through Fine-Tuning Gating Signals. , 2006, , .		1
745	A Modified Equivalent Circuit for Common-Mode Current of Single-Phase Full-Bridge Inverters. Industrial Electronics Society (IECON), Annual Conference of IEEE, 2006, , .	0.0	2
746	Common Mode EMI Suppression Based on Simulated Annealing Algorithm. , 2006, , .		3
747	One Cost-effective Feedback Control Scheme for PWM Inverters Based on Repetitive Control. , 2006, , .		2
748	Determination of trans-Resveratrol in China Great Wall â€~ã€~Fazenda'' Red Wine by Use of Micellar Electrokinetic Chromatography. Chromatographia, 2005, 62, 289-294.	1.3	14
749	Photon-by-Photon Determination of Emission Bursts from Diffusing Single Chromophores. Journal of Physical Chemistry B, 2005, 109, 21930-21937.	2.6	28
750	Direct repetitive control of SPWM inverter for UPS purpose. IEEE Transactions on Power Electronics, 2003, 18, 784-792.	7.9	342
751	Study on the mechanism of output waveform distortion and distortion suppression of PWM VSI with rectifier load. , 0, , .		0
752	Prediction of common mode conducted EMI in single phase PWM inverter. , 0, , .		8
753	State-feedback-with-integral control plus repetitive control for UPS inverters. , 0, , .		12
754	Traffic sign detection algorithm based on feature expression enhancement. Multimedia Tools and Applications, 0, , 1.	3.9	5
755	Stochastic model predictive control for spacecraft rendezvous and docking via a distributionally robust optimization approach. ANZIAM Journal, 0, 63, 39-57.	0.0	0
756	Understanding the current-voltage characteristic in HTS wires and bulks is of continuing interest to the modelling community. Superconductor Science and Technology, 0, , .	3.5	0